RADIOCARBON, Vol 46, Nr 3, 2004, p 1059–1086

MARINE04 MARINE RADIOCARBON AGE CALIBRATION, 0–26 CAL KYR BP

Konrad A Hughen[1] • Mike G L Baillie[2] • Edouard Bard[3] • J Warren Beck[4] • Chanda J H Bertrand[1] • Paul G Blackwell[5] • Caitlin E Buck[5] • George S Burr[6] • Kirsten B Cutler[7] • Paul E Damon[6] • Richard L Edwards[8] • Richard G Fairbanks[9] • Michael Friedrich[10] • Thomas P Guilderson[11,16] • Bernd Kromer[12] • Gerry McCormac[2] • Sturt Manning[13,14] • Christopher Bronk Ramsey[15] • Paula J Reimer[2,11] • Ron W Reimer[16] • Sabine Remmele[10] • John R Southon[17] • Minze Stuiver[18] • Sahra Talamo[12] • F W Taylor[19] • Johannes van der Plicht[20,21] • Constanze E Weyhenmeyer[11]

ABSTRACT. New radiocarbon calibration curves, IntCal04 and Marine04, have been constructed and internationally ratified to replace the terrestrial and marine components of IntCal98. The new calibration data sets extend an additional 2000 yr, from 0–26 cal kyr BP (Before Present, 0 cal BP = AD 1950), and provide much higher resolution, greater precision, and more detailed structure than IntCal98. For the Marine04 curve, dendrochronologically-dated tree-ring samples, converted with a box diffusion model to marine mixed-layer ages, cover the period from 0–10.5 cal kyr BP. Beyond 10.5 cal kyr BP, high-resolution marine data become available from foraminifera in varved sediments and U/Th-dated corals. The marine records are corrected with site-specific ^{14}C reservoir age information to provide a single global marine mixed-layer calibration from 10.5–26.0 cal kyr BP. A substantial enhancement relative to IntCal98 is the introduction of a random walk model, which takes into account the uncertainty in both the calendar age and the ^{14}C age to calculate the underlying calibration curve (Buck and Blackwell, this issue). The marine data sets and calibration curve for marine samples from the surface mixed layer (Marine04) are discussed here. The tree-ring data sets, sources of uncertainty, and regional offsets are presented in detail in a companion paper by Reimer et al. (this issue).

INTRODUCTION

Radiocarbon dates must be converted to calendar ages for greatest utility in comparison, for example, to known historical ages in archaeology or calendric ice cores and layer-counted marine sediments as well as U/Th chronologies in paleoceanographic studies. Tree-ring dendrochronologies provide the most accurate and highest resolution calibration data for terrestrial ^{14}C ages, but currently are limited to the past 12.4 cal kyr BP (Friedrich et al., this issue). In addition, for calibration of marine dates, tree-ring ^{14}C ages must be modeled to derive equivalent ocean mixed-layer ages.

[1]Woods Hole Oceanographic Institution, Department of Marine Chemistry & Geochemistry, Woods Hole, Massachusetts 02543, USA.
[2]School of Archaeology and Palaeoecology, Queen's University Belfast, Belfast BT7 1NN, United Kingdom.
[3]CEREGE, UMR-6635, Europole de l'Arbois BP80, 13545 Aix-en-Provence cdx 4, France.
[4]Department of Physics, University of Arizona, Tucson, Arizona 85721, USA.
[5]Department of Probability and Statistics, University of Sheffield, Sheffield S3 7RH, United Kingdom.
[6]Department of Geosciences, University of Arizona, Tucson, Arizona 85721, USA.
[7]U.S. Department of State, Office of Senior Coordinator for Nuclear Safety, 2201 C Street NW, Washington DC, USA.
[8]Department of Geology and Geophysics, University of Minnesota, Minneapolis, Minnesota, USA.
[9]Lamont-Doherty Earth Observatory of Columbia University, Palisades, New York 10964, USA.
[10]Universität Hohenheim, Institut für Botanik-210, D-70593 Stuttgart, Germany.
[11]Center for Accelerator Mass Spectrometry L-397, Lawrence Livermore National Laboratory, Livermore, California 94550, USA.
[12]Heidelberger Akademie der Wissenschaften, Im Neuenheimer Feld 229, D-69120 Heidelberg, Germany.
[13]The Department of Fine Art, Sidney Smith Hall, 100 St. George Street, University of Toronto, Ontario M5S 3G3, Canada.
[14]Department of Archaeology, University of Reading, P.O. Box 217 Whiteknights, Reading RG6 6AB, United Kingdom.
[15]Oxford Radiocarbon Accelerator Unit, 6 Keble Rd., Oxford OX2 6JB, England.
[16]Department of Ocean Sciences, University of California, Santa Cruz, California 92697, USA.
[17]Department of Earth System Science, University of California, Irvine, California 92697, USA.
[18]Quaternary Isotope Lab, University of Washington, Seattle, Washington 98195, USA.
[19]Institute for Geophysics, University of Texas, Austin, Texas, USA.
[20]Center for Isotope Research, Groningen University, 9747 AG Groningen, the Netherlands.
[21]Faculty of Archaeology, Leiden University, P.O. Box 9515, 2300 RA Leiden, the Netherlands.

High-resolution measurements of the marine ^{14}C calibration curve beyond tree rings have been obtained from planktonic foraminifera in layer-counted varved sediments, extending detailed calibration back to 14.7 cal kyr BP (Hughen et al. 2000). Additional marine data parallel to and beyond the varved sediment record are available through extensive measurements from U/Th-dated corals around the world (Edwards et al. 1993; Bard et al. 1998; Burr et al. 1998; Burr et al., this issue; Cutler et al., this issue; Fairbanks et al., forthcoming).

In this paper, we describe the data sets and methods used to construct the new internationally approved marine calibration curve known as Marine04. Details concerning the original tree-ring data used for the younger portion of Marine04, 0–10.5 cal kyr BP, are given in a companion paper by Reimer et al. (this issue). Because high-resolution marine data are lacking from 0 to 10.5 cal kyr BP, the calibration curve for surface mixed-layer marine samples, Marine04, is constructed over this period from tree-ring measurements (Figure 1). The tree-ring data are combined using a random walk model (RWM) described in detail in Buck and Blackwell (this issue). The IntCal04 tree-ring-based curve that is estimated by the random walk model is then used as input to a global ocean-atmosphere box diffusion model (Stuiver and Braziunas 1993). The model is used to deconvolve the ^{14}C production rate from the tree-ring data and calculate the "global" ocean mixed-layer ^{14}C ages. Beyond tree-rings, ^{14}C measurements of foraminifera from Cariaco Basin varved sediments and U-series dated corals are used to construct the calibration curve. The high-resolution Cariaco Basin data set begins at 10.5 cal kyr BP, and the tree-ring-based data set is therefore only used back to that time. The coral and foraminiferal ^{14}C data sets are converted to "global" ocean mixed-layer values by subtracting the difference (ΔR) between the regional reservoir age and the mixed-layer reservoir age R (Stuiver et al. 1986) calculated from the box diffusion model. The output from the global ocean-atmosphere box diffusion model and the normalized coral and foraminiferal ^{14}C data are then combined via the RWM to derive an estimate of the underlying marine curve. It is this estimate from the RWM which is continuous between 0 and 26 cal kyr BP that we call Marine04.

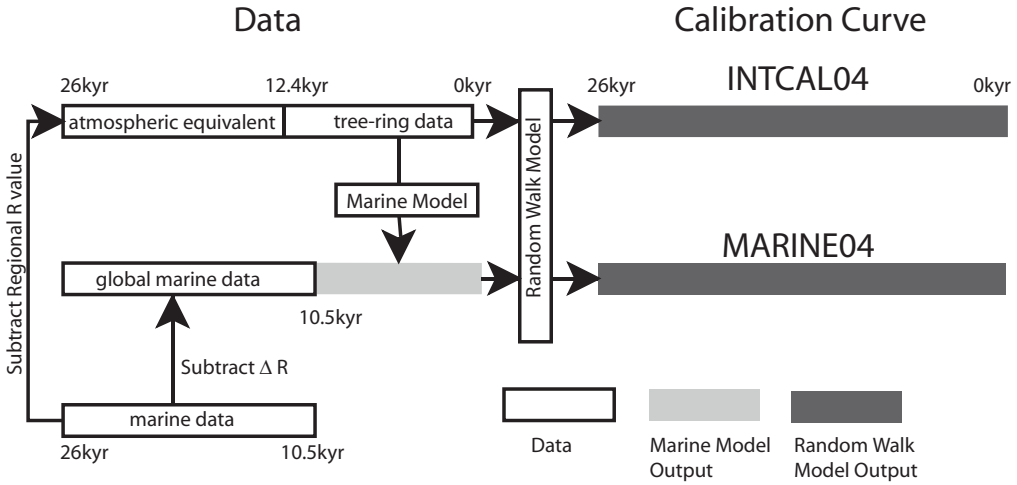

Figure 1 Schematic diagram of IntCal04 and Marine04 calibration data set construction. Tree-ring data extend from 0 to 12.4 cal kyr BP. Beyond the end of the tree rings, coral and foraminifera data are converted to the atmospheric equivalent by subtracting a site-specific reservoir correction R. These data are input into the random walk model (RWM) to produce IntCal04. Marine data from 10.5–26.0 cal kyr BP are normalized to the "global" ocean by subtracting ΔR, the regional difference from the model ocean reservoir age of 405 yr. The "global" marine data and the output from the box diffusion model (see main text) are used with the RWM to provide our estimate of the global marine calibration curve Marine04.

The IntCal04 working group, which met at Queen's University Belfast in April 2002 and at Woods Hole Oceanographic Institution in May 2003, established criteria for acceptance of data into the IntCal04 and Marine04 calibration data set including general limitations on analytical errors and acceptable scatter and specific record-dependent criteria (Reimer et al. 2002). The criteria for acceptable tree-ring records are discussed in brief in Reimer et al. (this issue). For corals, criteria were established to detect alteration of the original aragonite, including X-ray diffraction measurements to show <1% calcite, initial $\delta^{234}U$ within ±5‰ of accepted seawater values, and concordant protactinium ages where available, especially where diagenesis is most likely due to sub-aerial exposure. Numerous data from corals with pristine aragonite, and in several cases concordant Pa ages, have led to a revision in our understanding of the history of seawater $\delta^{234}U$ (see Cutler et al., this issue and references therein), and adoption of new criteria for coral initial $\delta^{234}U$ values. These criteria are discussed in greater detail in a later section. For layer-counted chronologies, such as those based on varve counting, acceptance criteria include the need for multiple-core chronologies to confirm that no sections are missing from core-breaks or erosion. In addition, independent radiometrically-dated tie points should be employed whenever possible to validate and assess the quality of the layer chronology. For all marine records, site-specific reservoir corrections should be measured, and a "reasonable" error should be reported with the reservoir age (Reimer et al. 2002).

The calibration data sets for terrestrial and marine samples were presented for ratification at the 18th International Radiocarbon Conference in Wellington, New Zealand in September 2003. Suggestions from conference participants have been incorporated into the final product. We do not make a recommendation for calibration beyond 26 kyr at this time due to large disparities between the available data sets (van der Plicht et al., this issue).

THE MARINE04 DATA SETS

The data sets used in the IntCal04 and Marine04 calibrations are given in full as supplemental material on the *Radiocarbon* Web site (www.radiocarbon.org) and are also available at www.calib.org. Uncertainties are given for the ^{14}C ages and for the calibrated or cal time scales in order that they both may be accounted for in the curve building process (see Buck and Blackwell, this issue). Replicate ^{14}C measurements within a laboratory or made by two or more laboratories are given separately, when available. These data are not necessarily completely independent estimates of the underlying calibration curve, since they are derived from the same samples, but have been included for completeness.

Tree-Ring Data Sets (0–10.5 cal kyr BP)

The Holocene part of the Marine04 ^{14}C calibration is based on several millennia-long tree-ring chronologies, providing an annual, nearly absolute time frame, which was rigorously tested by internal replication of many overlapping sections. Whenever possible, chronologies were cross-checked with independently established chronologies of adjacent regions. Details of individual tree-ring data sets are provided by Reimer et al. (this issue).

Marine Data Sets (10.5–26 cal kyr BP)

Marine calibration older than 10.5 cal kyr BP is provided by data from Cariaco Basin and coral U/Th ages. Cariaco and coral data are combined from 10.5 to 14.7 cal kyr BP, and coral data alone are used to extend calibration back to 26 cal kyr BP. We calculated site-specific reservoir corrections from the weighted mean difference of marine and tree-ring ^{14}C ages using data overlapping from 500–12,500 BP (Table 1), not including recent pre-bomb data pairs used in previous publications. This was done in order to avoid uncertainty in the degree of fossil fuel influence on reservoir calcu-

lations from recent samples, and also to assess changes in reservoir age due to different climatic states (e.g. Younger Dryas). In addition, the increased number of marine-terrestrial age comparisons provides more realistic error estimates on calculated reservoir corrections. For each marine sample, the difference in ^{14}C age was calculated for the point in the tree-ring-derived portion of IntCal04 nearest to it in time. For this comparison, no error was included for the calendar age of the marine samples. However, the IntCal04 curve was smoothed with a 20-point (100-yr) average to diminish the influence of calendar age uncertainty. The variance of the difference was calculated as the sum of the squared errors of the marine and the IntCal04 ^{14}C ages. The weighted mean of all the differences was calculated for each location and the observed standard deviation was taken as the uncertainty (Table 1). For the Vanuatu corals, a decadal average of the Burr et al. (1998) single-year data was used for the comparison in addition to the Cutler et al. (this issue) data. For Mururoa, there are no overlapping tree-ring data points, so we use the value calculated for Tahiti, which is within a reasonable proximity. The calendar chronology for Cariaco Basin is based on a wiggle-match with the tree-rings, so there is obvious circularity in using this difference, although the calculated value overlaps with measurements from the core top (Hughen et al. 1996) and from corals from Isla Tortugas (Guilderson et al., forthcoming). For all sites, the reservoir corrections calculated here agree well within errors with previous measurements (Table 1). For sites where we have compiled modern "pre-bomb" data (<100 BP), the inclusion of a fossil fuel correction (Bard et al. 1988; Southon et al. 2002; Guilderson et al., forthcoming) may change calculated reservoir ages by up to 100 yr, although are generally still in agreement with the new values.

The current state of knowledge dictates that for construction of a global marine ^{14}C calibration curve, site-specific reservoir and ΔR values are assumed to be constant with time. Although there is evidence for large (factor of two) reservoir age shifts in the past—e.g., during deglaciation in the high-latitude North Atlantic (Bard et al. 1994; Austin et al. 1995; Bjork et al. 1998; Bondevik et al. 1999; Eiriksson et al. 2000; Waelbrook et al. 2001), Mediterranean Sea (Siani et al. 2001), and New Zealand region (Sikes et al. 2000)—all marine data sets used in Marine04 come from low-latitude tropics where the fluctuations in reservoir correction may not be as great. For example, Cariaco Basin ^{14}C ages agree closely with anchored tree-ring ages from 10.5 to 12.4 cal kyr BP across the large climatic shifts of the Younger Dryas (Hughen et al., this issue), exhibiting no evidence of significant reservoir variability. Nevertheless, the Cariaco comparison to floating tree-ring sections indicates the possibility that reservoir age increased by up to 50% during the Allerød (Kromer et al., this issue). Therefore, both within single locations and between regions, some changes in reservoir correction through time may be apparent—either as slight trends or increased/decreased variability (Figure 2). Many of these changes reflect real shifts in regional or local oceanography, such as surface circulation and advection, meridional overturning, or local upwelling, rather than analytical uncertainties due to sample diagenesis or laboratory error. For example, the large variability in the Papua New Guinea and Vanuatu reservoir calculations are probably indications of changes in the amount of Eastern Equatorial water reaching these sites and local upwelling at Papua New Guinea. The Papua New Guinea coral data of Burr et al. (this issue), in comparison with the other marine data sets (Figure A7), could be used to argue for a smaller reservoir correction than either the known-age pre-bomb value of Edwards et al. (1993) or our calculation from the tree-ring overlap (Table 1), which underscores the high reservoir variability at this site.

Quantifiable records of changes in regional oceanographic conditions adequate for predicting and correcting such reservoir variability are presently lacking. Thus, a certain degree of scatter in site-specific reservoir values through time cannot be avoided, and must instead be characterized as reservoir uncertainty. This uncertainty incorporates all sources of error in reservoir measurement and

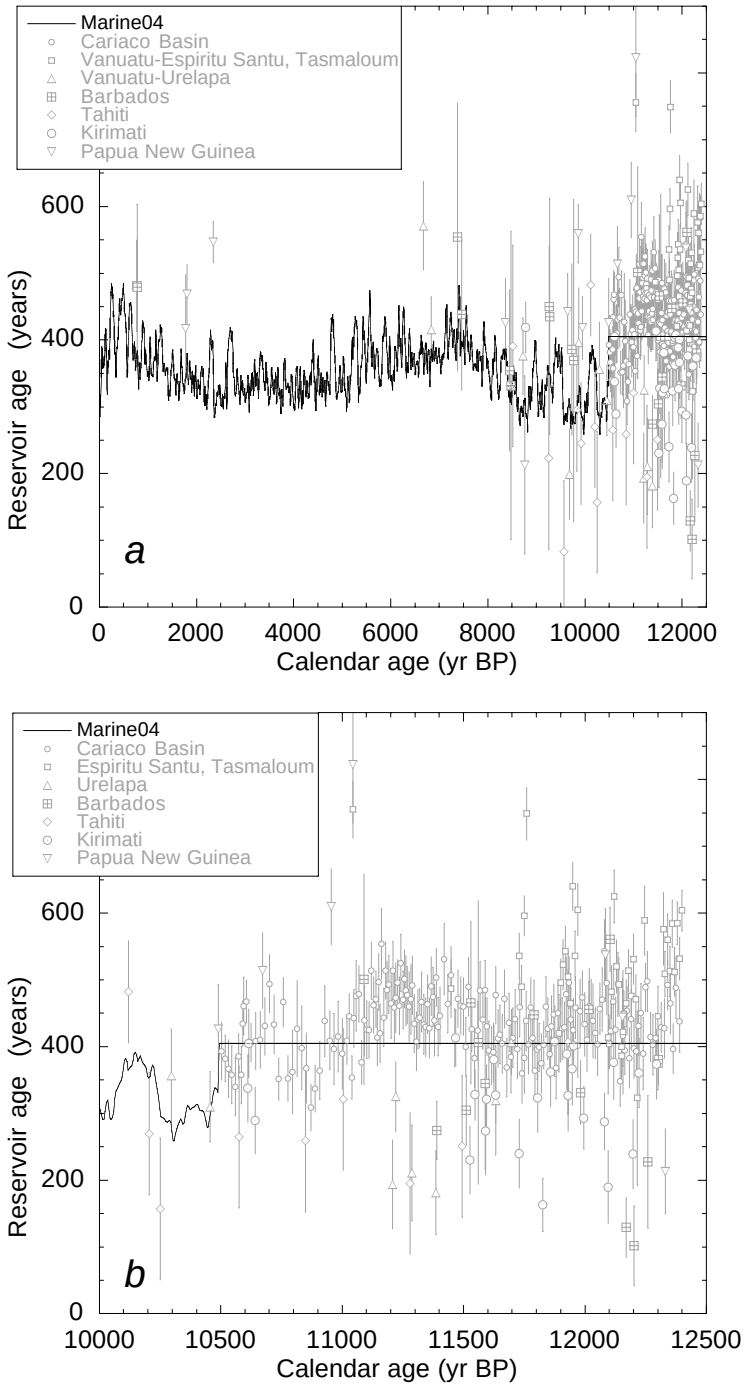

Figure 2 Site-specific reservoir corrections for the locations used in IntCal04 and Marine04. Sites include Cariaco Basin (Hughen et al., this issue); Vanuatu (Burr et al. 1998; Cutler et al., this issue); Barbados (Bard et al. 1998; Fairbanks et al., forthcoming); Tahiti (Bard et al. 1998); Kirimati (Fairbanks et al., forthcoming); and Papua New Guinea (Edwards et al. 1993; Cutler et al., this issue). (a) Reservoir corrections from 0–12.5 cal kyr BP. Marine04 reservoir *R* changes from 0–10.5 due to shifts in atmospheric ^{14}C production, but is held constant beyond 10.5. (b) Blow-up of interval of greatest marine-terrestrial data overlap. Slight but coherent changes in reservoir age through time are likely due to real changes in oceanographic conditions (see text).

calculation, and is likely an overestimation of true oceanic variability. Increased data density in the future may allow us to identify spatial and temporal patterns of reservoir variability, increasing precision for calibration as well as our understanding of ocean circulation change.

Table 1 New and previously determined site-specific marine reservoir corrections.

Location	Reservoir correction (tree-ring overlap) ^{14}C yr	Uncertainty	*N*	Previous value (known age, "pre-bomb") ^{14}C yr
Barbados	360	80	22	400[a]
Cariaco Basin	430	30	196	420[b]
Kirimati	330	80	27	300
Mururoa	Same as Tahiti			
Papua New Guinea	490	150	17	407[c]
Tahiti	280	120	22	300[a]
Vanuatu	530	105	41	
Espiritu Santu				494[d]
Tasmaloum				500[d,e]
Vanuatu	350	120	14	
Urelapa				400[e]

[a]Bard et al. 1998.
[b]Hughen et al. 1996.
[c]Edwards et al. 1993.
[d]Burr et al. 1998.
[e]Cutler et al., this issue.

U/Th-Dated Corals

Mass spectrometric techniques have been used to measure paired ^{14}C and ^{230}Th (as well as ^{231}Pa) ages on fossil corals for ^{14}C calibration. A plot of coral initial δ^{234}U versus calendar age for corals which pass the <1% calcite criteria shows a distinct decline back in time (Figure 3). Adopting a screening criteria based on modern seawater δ^{234}U of 145.8 ± 5‰ (Cheng et al. 2000) as originally proposed would eliminate approximately half of the data between 17 and 26 cal kyr BP. Many of the older coral data show concordant ^{231}Pa ages (Cutler et al., this issue; Fairbanks et al., forthcoming), and thus the lower value for initial δ^{234}U is probably a reflection of true changes in seawater δ^{234}U through time. We set the acceptance criteria to be within 3 standard deviations of the mean value for the 2 groups of corals before and after 17 cal kyr BP. For corals that grew from 0–17 cal kyr BP, initial δ^{234}U must lie within ± 7.2‰ (3 σ) of 145.2‰ (n = 171), close to our original criteria of accepted seawater values. However, for older corals between 17 and 26 cal kyr BP in age, initial δ^{234}U appears to be lower and a new value has been adopted for screening, 140.6 ± 7.2‰ (3 σ, n = 80) (see Figure 3). Although the data in Figure 3 could also accommodate a gradually changing seawater δ^{234}U, it is possible that seawater δ^{234}U may have changed abruptly following input of high ^{234}U/^{238}U glacial flour during deglaciation (e.g. Robinson et al. 2004). Thus, a two-step model is used here for simplicity.

The data sets of Bard et al. (1990, 1998), Edwards et al. (1993), and Burr et al. (1998) were used in IntCal98 (Stuiver et al. 1998) and have been updated for inclusion in IntCal04 and Marine04. Extensive new coral data sets have been included from Cutler et al. (this issue) and Fairbanks et al. (forthcoming).

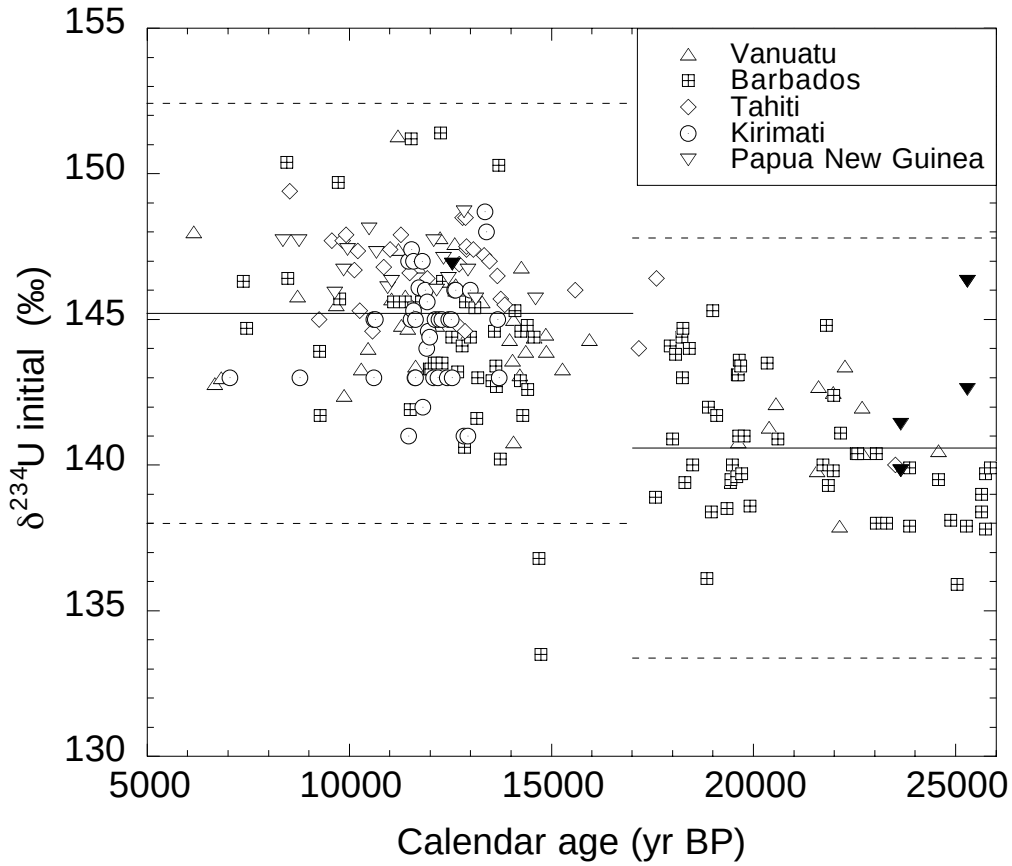

Figure 3 Initial $\delta^{234}U$ calculated from coral calibration data from 0–26 cal kyr BP. Symbols and references for sites are the same as in Figure 2. The data show a general decrease in initial $\delta^{234}U$ for the earlier interval, 17–26 cal kyr BP, although some data points possess concordant ^{231}Pa ages (solid symbols). A lower value for initial $\delta^{234}U$, 140.6 ± 7.2‰ (3 σ), has therefore been adopted as part of the acceptance criteria for corals older than 17 cal kyr BP, and a value of 145.2 ± 7.2‰ (3 σ) for corals younger than 17 cal kyr BP.

Bard et al. (1998) collected samples from boreholes drilled off the islands of Tahiti and Mururoa, French Polynesia, in order to complement the database previously obtained on Barbados corals (Bard et al. 1990, 1993). Nineteen dates from Barbados cover an age span from 0.7 to 22 cal kyr BP; 27 dates from Tahiti cover 9.5 to 13.8 cal kyr BP; 4 dates from Mururoa span 15.5 to 23.5 cal kyr BP.

Edwards et al. (1993) measured paired ^{14}C and ^{230}Th ages on uplifted fossil corals from the Huon Peninsula, Papua New Guinea. Seventeen age pairs cover an age span from 7.6 to 13.1 cal kyr BP. Revised ^{234}U and ^{230}Th half-lives for ^{230}Th-age and $\delta^{234}U$ (Cheng et al. 2000) have been applied.

Burr et al. (1998) analyzed a single *Diploastrea heliopora* coral from Vanuatu. Growth bands in the coral were used to identify individual years of growth. ^{14}C measurements were made on each year and are updated here to the original annual resolution; 352 dates over 4 discrete intervals cover an age span between 11.7 and 12.4 cal kyr BP. Burr et al. (this issue) analyzed a single *Goniastrea favulus* coral from drilling which took place on an uplifted Holocene terrace on the Huon Peninsula, Papua New Guinea, in the age range of 13.0 and 13.1 cal kyr BP in 6-month growth intervals.

Cutler et al. (this issue) analyzed fossil corals in drill cores from Papua New Guinea and Vanuatu, obtaining calendar ages using both ^{230}Th and ^{231}Pa dating techniques. Six samples from Papua New Guinea span an age range from 12.4 to 25.3 cal kyr BP; 48 samples were obtained from Vanuatu—25 dates from Tasmaloum spanning ages of 11.0 to 24.6 cal kyr BP, and 23 dates from Urelapa covering ages from 5.4 to 19.6 cal kyr BP. ^{231}Pa was measured for 11 samples from Papua New Guinea (18 measurements) and eight of those samples were found to be concordant. These measurements are shown as solid triangles in Figure 3.

Fairbanks et al. (forthcoming) recovered drill cores from Barbados and Kirimati in the Caribbean and central Pacific. Dating with ^{238}U/^{234}U/^{230}Th used a multi-collector magnetic sector ICP mass spectrometer: 190 dates from Barbados cover an age range from 0.7 to 25.8 cal kyr BP, and 64 dates from Kirimati span ages from 7.0 to 13.7 cal kyr BP. ^{231}Pa was measured for a number of samples with low initial δ^{234}U (Fairbanks et al., forthcoming).

Cariaco Basin Varved Sediments

For the IntCal98 data set (Stuiver et al. 1998), high-resolution calibration data older than tree rings were provided by Cariaco Basin piston core PL07-PC56 (Hughen et al. 1998). Core 56PC was sampled every 10 cm, yielding approximately 100–200 yr resolution. For this IntCal04 curve, data are used from Cariaco piston core PL07-58PC, with a ~25% higher deposition rate than 56PC. Core 58PC was sampled every 1.5 cm, providing ^{14}C calibration at 10–15 yr resolution throughout the period of deglaciation (Hughen et al. 2000). The floating Cariaco varve chronology was anchored to the revised and extended German pine chronology (Friedrich et al., this issue) by wiggle-matching detailed ^{14}C structure over a 1900-yr window (Hughen et al., this issue); 388 dates span an age range from 10.5 to 14.7 cal kyr BP.

Sources of Uncertainty

In cases where replicate ^{14}C analyses have been made, it is possible to examine the actual variability in sample preservation, preparation, and measurement, and thus estimate an error multiplier by which the nominal laboratory error should be increased to allow for all additional sources or error. We compared the replicate analyses of Polynesian corals measured at the Gif-sur-Yvette AMS facility (Bard et al. 1998; Paterne et al. 2004; Bard et al., this issue). The average nominal error in the 9 replicated observations was 95 ^{14}C yr, whereas the observed standard deviation was 142 ^{14}C yr. Therefore, an error multiplier of 1.5 appears to be appropriate. We also compared replicate measurements of Barbados and Kirimati corals measured at CAMS (Fairbanks et al., forthcoming). For 118 replicates, individual samples of coral were leached, graphitized, and analyzed. The average standard deviation in the difference was 24 ^{14}C yr and the observed standard deviation was 19 ^{14}C yr, which gives an error multiplier of 0.8, rounded up to 1.0. The coral data measured at the NSF-Arizona AMS Laboratory were previously determined to have a multiplier of 1.0 (Donahue et al. 1997), and this value was used for all Arizona AMS coral measurements. For the remaining coral data, an error multiplier of 2.0 was used as a conservative way to ensure that allowance is made for variability beyond the nominal laboratory error. In comparing these values with the existing literature, it is important to note that for corals, it has been customary to report the uncertainty at the 2-standard deviation level (Edwards et al. 1993; Bard et al. 1998).

For Cariaco Basin forams, 80 replicate samples were picked, cleaned, and analyzed. The average standard deviation in the difference was 42 ^{14}C yr and the observed standard deviation was 28 ^{14}C yr, which gives an error multiplier of 0.7, rounded up to 1.0. Another representation of ^{14}C reproducibility for Cariaco samples can be obtained by the results of 28 measurements of the foram-rich

TIRI/FIRI turbidite sample made at the CAMS laboratory where the Cariaco samples were measured (Guilderson et al. 2003), and from the comparison of ^{14}C measurements between Cariaco foraminifera and tree rings (Hughen et al., this issue). In both of these cases, the observed standard deviation of the measurements is consistent with the uncertainty estimates derived from measurement error and background-correction uncertainties.

CALIBRATION CURVE CONSTRUCTION

The Marine04 curve is constructed in 2 parts using a combination of tree-ring and marine data sets (Figure 1). From 0–10.5 cal kyr BP, where high-resolution marine data are lacking, Marine04 uses the dendrochronology-based curve of IntCal04. The tree-ring data are used along with the random walk model (RWM) detailed in Buck and Blackwell (this issue) to provide an estimate of the underlying atmospheric calibration curve, known as IntCal04. This curve is then converted with an ocean-atmosphere box diffusion model to yield ocean mixed-layer ^{14}C ages. The mixing and decay time of ^{14}C in the oceans slightly smoothes and attenuates the output of the box diffusion model, which is offset from the atmospheric IntCal04 curve by a global mixed-layer reservoir age *R* (Figure 4a). The "global" reservoir ^{14}C age of the surface ocean, R(t), is the time-dependent difference between the modeled or measured "global" surface ocean and atmospheric ^{14}C ages. From 0–12.4 cal kyr BP, where both tree-ring and calculated mixed-layer ages exist, *R* varies with time as a result of rapid shifts in atmospheric $\Delta^{14}C$ being attenuated in the surface ocean (Figure 4b). Beyond 10.5 cal kyr BP, Marine04 relies on direct measurements of marine ^{14}C ages from corals and foraminifera. Individual marine data sets were corrected to a consistent global mixed-layer ^{14}C data set by subtracting ΔR. ΔR is defined as the difference between the regional surface ocean ^{14}C age and the "global" surface ocean ^{14}C age (Stuiver et al. 1986). Because atmospheric forcing of the regional part of the ocean and the world ocean are approximately parallel, ΔR, for a given region, can, as a first approximation, be assumed to be constant. However, changes in oceanic circulation patterns or regional upwelling of deep (older) water may cause ΔR to vary with time. Whether or not ΔR for a given region is constant through time is thus an important issue when establishing a chronology for marine records or calibrating marine ^{14}C ages. A global *R* value for the period 10.5–26 cal kyr BP was determined by the results of box diffusion model simulations for 500 yr from AD 1350–1850 (described below), and equaled 405 ± 22 yr. The uncertainty in the corrected "global" marine data set was calculated from the uncertainties in the marine ^{14}C uncertainty and ΔR combined in quadrature, neglecting the box diffusion model uncertainty. The corrected "global" marine data and the output from the box diffusion model were then combined via the RWM to obtain our estimate of the global marine calibration curve, Marine04 (Figure 5).

To calibrate marine ^{14}C ages using Marine04, one must know ΔR, the site-specific offset from the global ocean reservoir. Although global *R* in Marine04 changes from 0–10.5 cal kyr BP (but remains constant from 10.5–26 cal kyr BP), it is assumed that ΔR for any given marine location remains constant to a first approximation. To calculate ΔR, the site-specific marine ^{14}C age is compared to the Marine04 mixed-layer ^{14}C age for any known calendar age. For modern pre-bomb measurements, the calendar age is usually known or can be estimated accurately. A database of ΔR values calculated for known-age marine samples is maintained at www.calib.org/marine. To evaluate the assumption of constant ΔR further back in time, terrestrial-marine pairs may be dated; however, great care must be taken to ensure that they are indeed contemporaneous. In those cases, ΔR can be calculated either by calibrating the terrestrial ^{14}C age and comparing the difference between the equivalent marine age and the measured marine age (Southon et al. 1995) or by directly comparing the terrestrial ^{14}C age and the marine age using the combined IntCal04-Marine04 data set following the method of Stuiver and Braziunas (1993) and Reimer et al. (2002b). ΔR and its estimated uncertainty is then used in conjunction with the marine calibration curve in most calibration software.

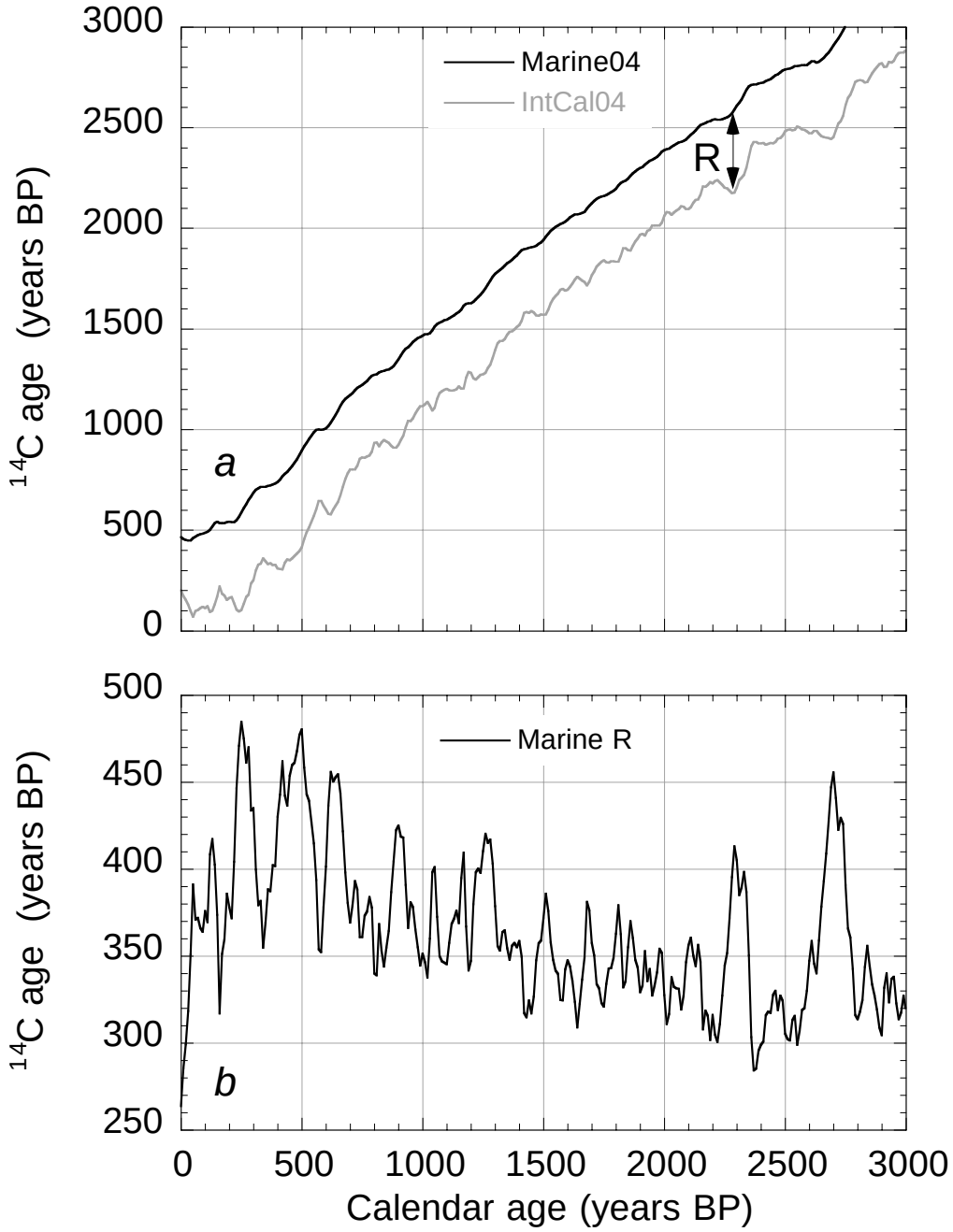

Figure 4 Global marine reservoir age "R" for the past 3000 yr. Atmospheric ^{14}C changes quickly following production spikes, but is muted in the ocean mixed layer. As a result, *R* calculated by the difference between IntCal04 and box diffusion model output (curve a) shows large variability (curve b). Beyond 10.5 cal kyr BP, when the Marine04 curve relies entirely on marine ^{14}C data sets, the global reservoir *R* is held constant at 405 yr (see Figure 2).

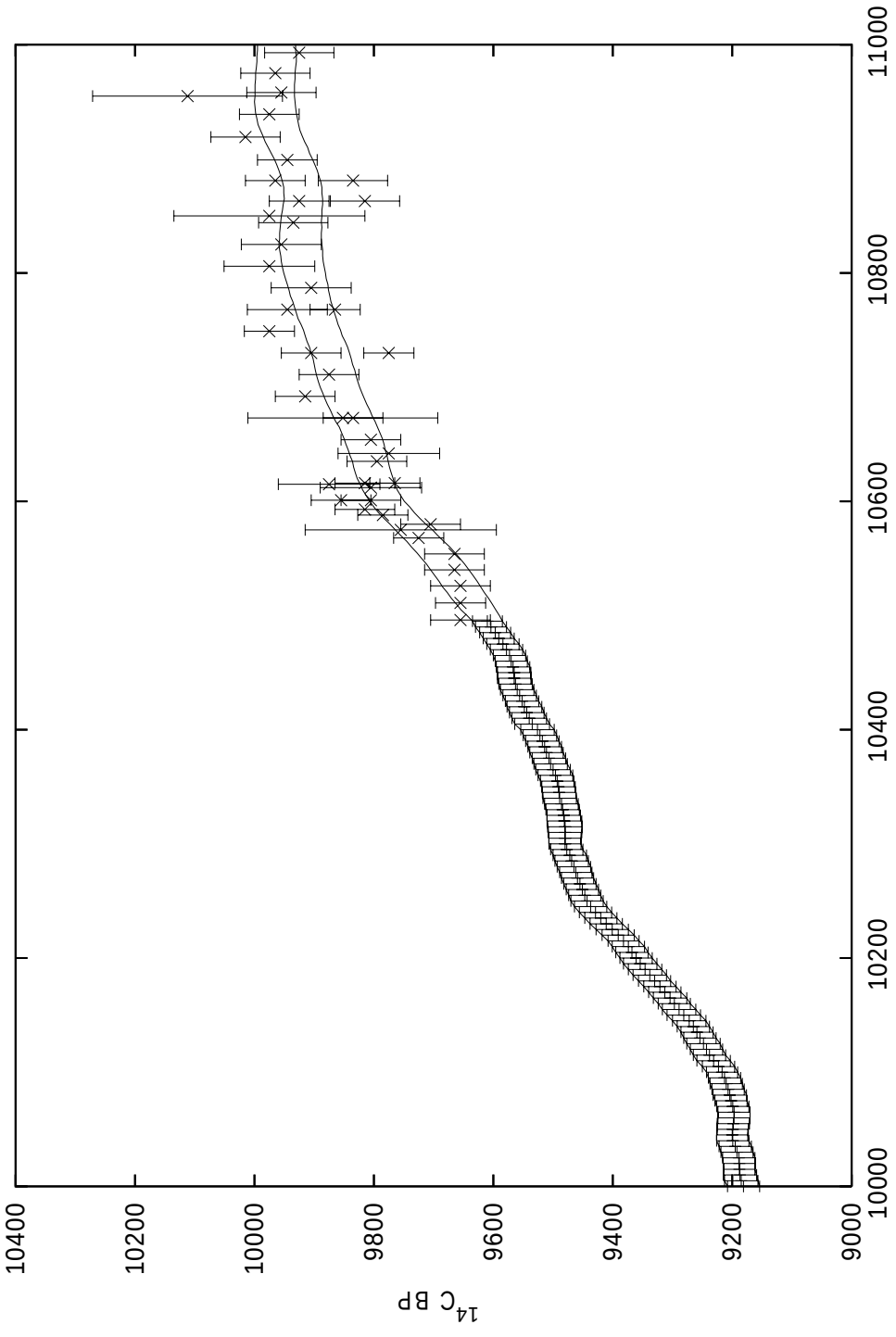

Figure 5 Close-up of the transition between tree-ring-based and marine-based sections of the Marine04 curve. Although global *R* (for calculating marine data $\Delta R > 10.5$ cal kyr BP) is taken from the box diffusion model output between AD 1300–1800, the box diffusion model output of tree-ring data also shows a smooth transition to the RWM output of marine data sets at 10.5 cal kyr BP.

Random Walk Model

For IntCal04 and Marine04, the calendar age span (e.g. number of tree rings, varves, or coral growth bands) and calendar age uncertainty of the samples is taken into account through a stochastic random walk model (RWM) that estimates the underlying ^{14}C calibration curve (Buck and Blackwell, this issue). This model assumes that the changes in the curve from one year to the next can be represented by a Gaussian distribution. Details of the RWM and of the selection of the necessary parameters are given in Buck and Blackwell (this issue). The Marine04 ^{14}C calibration curve is estimated and reported here at intervals of 5 yr for the range 0–10 cal kyr BP, 10 yr for 10–15 cal kyr BP, and 50 yr for 15–26 cal kyr BP.

Ocean-Atmosphere Box Diffusion Model

The ocean-atmosphere box diffusion model is based on the work of Oeschger et al. (1975). The model was parameterized to produce a pre-industrial marine mixed-layer $\Delta^{14}C$ of –46.5‰ and a deep-ocean value of –190‰ at AD 1830 for the 1998 marine calibration data set, Marine98 (Stuiver et al. 1998b). This resulted in a reservoir age of 390 ^{14}C yr for AD 1830 and an average reservoir age of 360 for the period 7050 BC to AD 1850 when compared to the atmospheric values from IntCal98. For Marine04, we used IntCal04 from 0–12.4 kyr for input and allowed the model to spin up with the initial conditions for 2000 yr to bring the system to equilibrium. The air-sea gas exchange coefficient F and eddy diffusivity K_z were varied slightly (Table 2) to achieve the Marine98 $\Delta^{14}C$ values for the mixed layer over the last 500 yr. Initial atmospheric $\Delta^{14}C$ was set to 100‰, the average value at the beginning of the tree-ring data set. Pre-industrial atmospheric CO_2 concentration was set slightly lower at 270 ppm based on measurements of CO_2 trapped in ice from Law Dome, Antarctica (Indermuhle 2000); however, the model is relatively insensitive to changes in atmospheric CO_2 concentration of this order of magnitude. All other parameters were unchanged from Marine98. A representative section of the atmospheric ^{14}C record and box diffusion model mixed layer are shown in Figure 4.

Table 2 Box diffusion model parameters for Marine98 versus Marine04.

Parameter	Marine98	Marine04
Air-gas sea exchange	19 moles/m^2/yr	18.8 moles/m^2/yr
Eddy diffusivity	4000 m^2/yr	4220 m^2/yr
Pre-industrial atmospheric [CO_2]	280 ppm[a]	270 ppm
Biosphere residence time and reservoir size (fraction of the atmosphere)	2.7 yr; 0.34 atm 80 yr; 2.86 atm[b]	same
Ocean CO_2 concentration	2.31 mol/m^3[c]	same
Initial atmospheric $\Delta^{14}C$	90‰	100‰

[a]Neftel et al. 1985; Stuiver et al. 1984.
[b]Emanuel et al. 1984.
[c]Takahashi et al. 1981.

In Marine98, the uncertainty in the marine calibration data set was taken from the atmospheric data set, with no added uncertainty due to the choice of model parameters. We investigated the uncertainty in the box diffusion model by varying F and K_z within reasonable ranges. Using a simulation with 40,000 random normal deviates of F with mean 18.8 and standard deviation 1 moles/m^2/yr, and of K_z with mean 4220 and standard deviation 500 m^2/yr, the model produced a distribution for the offset between the surface mixed layer and the atmosphere with mean –50.4 and a standard deviation of 2.7‰, or for the reservoir correction with mean 405 and a standard deviation of 22 yr from AD 1350–1850. The value of 22 yr for the uncertainty on the box diffusion model is added in quadrature to the atmospheric data set uncertainty to yield the standard deviation for Marine04 from 0 to 10.5 cal kyr BP.

COMPARISON TO MARINE98

The new Marine04 calibration curve shows many improvements over the previous Marine98 curve. Substantial new data sets provide additional calibration back to 26 cal kyr BP (Cutler et al., this issue; Fairbanks et al., forthcoming), and higher-resolution coverage for the interval beyond tree rings >10.5 cal kyr BP (Hughen et al., this issue). As a result, Marine04 defines a great deal of structure beyond 15 cal kyr BP, whereas Marine98 essentially followed a straight line (Figure 6). Despite the increased ^{14}C uncertainty used here, resulting from included uncertainty in reservoir corrections, the increased data resolution and RWM methodology create a much smaller error envelope in the final curve (Figure 6). During the deglacial interval of rapid climate change, large uncertainties and ^{14}C reversals that were primarily the result of the Marine98 splining procedure resulted in a curve of little practical use. In contrast, the Marine04 curve shows more monotonic behavior and a smaller error envelope, much more useful for calibration during this important time period.

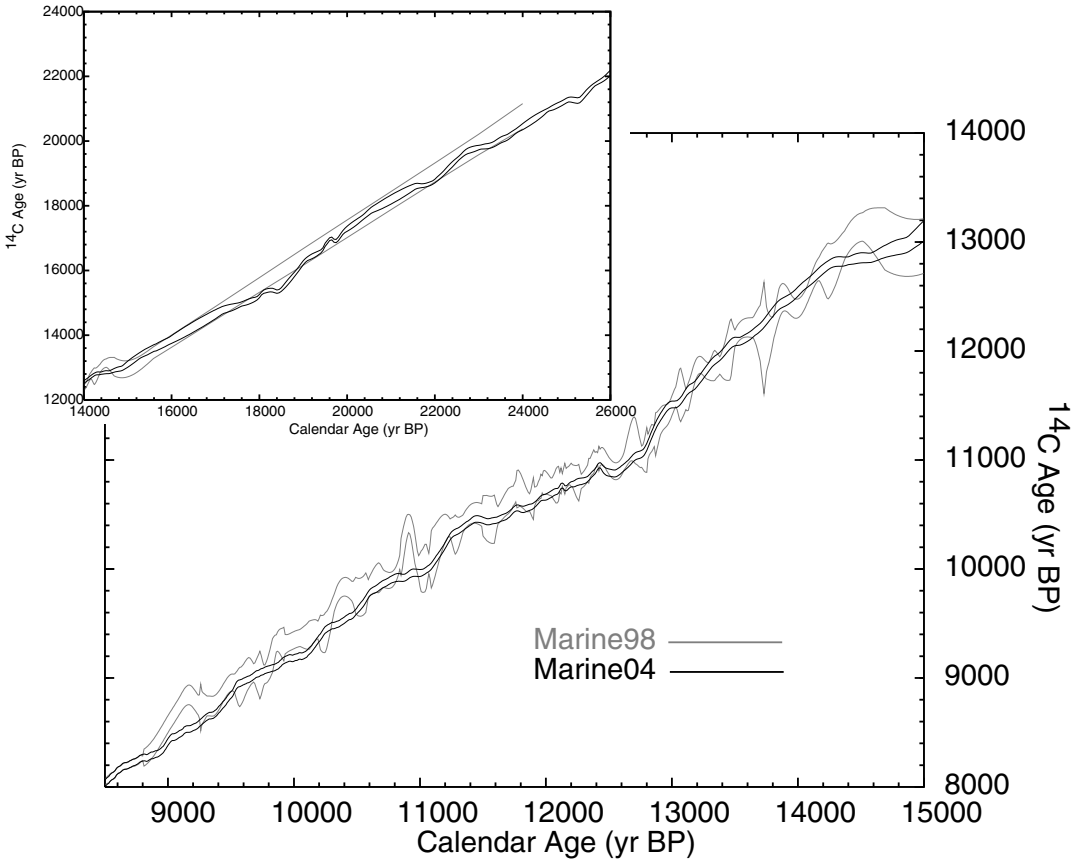

Figure 6 Comparison of Marine98 and Marine04 curves for interval beyond tree rings. Major improvements are evident during the interval of deglaciation, 15–10 cal kyr BP, and the Glacial period beyond 15 cal kyr BP (inset).

ACKNOWLEDGMENTS

We wish to thank the Leverhulme Trust for support for the IntCal workshops and a portion of the work on data compilation. We also thank Prof Gerry McCormac of the Queen's University Belfast

Radiocarbon Lab and Prof John Hayes of the National Ocean Sciences AMS Facility at Woods Hole Oceanographic Institution for generous hospitality and support in hosting the meetings. A portion of this work was performed under National Science Foundation grant ATM-0407554. A portion of this work was performed under the auspices of the U S Department of Energy by the University of California, Lawrence Livermore National Laboratory under Contract No. W-7405-Eng-48. This is WHOI contribution #11176.

Caitlin Buck acknowledges, with gratitude, the support and encouragement of her colleagues during a period of ill health while working on this project. In addition, she wishes to thank the staff of the Access to Work team in Sheffield and the Support Worker whom they funded, Sammy Rashid, without whose patience and practical and intellectual input she could not have completed her contribution to this work.

REFERENCES

Austin WEN, Bard E, Hunt JB, Kroon D, Peacock JD. 1995. The ^{14}C age of the Icelandic Vedde ash—implications for Younger-Dryas marine reservoir age corrections. *Radiocarbon* 37(1):53–62.

Bard E, Arnold M, Östlund HG, Maurice P, Monfray P, Duplessy J-C. 1988. Penetration of bomb radiocarbon in the tropical Indian Ocean measured by means of accelerator mass spectrometry. *Earth and Planetary Science Letters* 87:379–89.

Bard E, Hamelin B, Fairbanks RG. 1990. U-Th ages obtained by mass spectrometry in corals from Barbados; sea level during the past 130,000 years. *Nature* 346: 456–8.

Bard E, Arnold M, Fairbanks RG, Hamelin B. 1993. ^{230}Th-^{234}U and ^{14}C ages obtained by mass spectrometry on corals. *Radiocarbon* 35(1):191–9.

Bard E, Arnold M, Mangerud J, Paterne M, Labeyrie L, Duprat J, Melieres M-A, Sonstegaard E, Duplessy J-C. 1998. The North Atlantic atmosphere-sea surface ^{14}C gradient during the Younger Dryas climatic event. *Earth and Planetary Science Letters* 126:275–87.

Bard E, Ménot-Combes G, Rosek F. 2004. Present status of radiocarbon calibration and comparison records based on Polynesian corals and Iberian Margin sediments. *Radiocarbon*, this issue.

Bjorck S, Bennike O, Possnert G, Wohlfarth B, Digerfeldt G. 1998. A high-resolution ^{14}C-dated sediment sequence from southwest Sweden: age comparisons between different components of the sediment. *Journal of Quaternary Science* 13:85–9.

Bondevik S, Birks HH, Gulliksen S, Mangerud J. 1999. Late Weichselian marine ^{14}C reservoir ages at the western coast of Norway. *Quaternary Research* 52: 104–14.

Buck CE, Blackwell PG. 2004. Formal statistical models for estimating radiocarbon calibration curves. *Radiocarbon*, this issue.

Burr GS, Beck JW, Taylor FW, Recy J, Edwards RL, Cabioch G, Correge T, Donahue DJ, O'Malley JM. 1998. A high-resolution radiocarbon calibration between 11,700 and 12,400 calendar years BP derived from ^{230}Th ages of corals from Espiritu Santo Island, Vanuatu. *Radiocarbon* 40(3):1093–1105.

Burr GS, Galang C, Taylor FW, Gallup CD, Edwards RL, Cutler KB, Quirk B. 2004. Radiocarbon results from a 13-kyr BP coral from the Huon Peninsula, Papua New Guinea. *Radiocarbon*, this issue.

Cheng H, Edwards RL, Hoff J, Gallup CD, Richards DA, Asmerom Y. 2000. The half-lives of ^{234}U and ^{230}Th. *Chemical Geology* 169:17–33.

Cutler KB, Gray SC, Burr GS, Edwards RL, Taylor FW, Cabioch G, Beck JW, Récy J, Cheng H, Moore J. 2004. Radiocarbon calibration to 50 kyr BP with paired ^{14}C and ^{230}Th dating of corals from Vanuatu and Papua New Guinea. *Radiocarbon*, this issue.

Donahue DJ, Linick TW, Jull AJT. 1990. Isotope-ratio and background corrections for accelerator mass spectrometry radiocarbon measurements. *Radiocarbon* 32(2):135–42.

Edwards RL, Beck JW, Burr GS, Donahue DJ, Chappell JMA, Bloom AL, Druffel ERM, Taylor FW. 1993. A large drop in atmospheric ^{14}C/^{12}C and reduced melting in the Younger Dryas, documented with ^{230}Th ages of corals. *Science* 260:962–8.

Eiriksson J, Knudsen KL, Haflidason H, Heinemeier J. 2000. Chronology of late Holocene climatic events in the northern North Atlantic based on AMS ^{14}C dates and tephra markers from the volcano Hekla, Iceland. *Journal of Quaternary Science* 15:573–80.

Emanuel WR, Killough GG, Post WM, Shugart HH, Stevenson MP. 1984. Computer implementation of a globally averaged model of the world carbon cycle. Washington, DC: U S Dept of Energy, Carbon Dioxide Research Division Report. DOE/NBB-0062. 79 p.

Fairbanks RG, Mortlock RA, Chiu T-C, Guilderson TP, Cao L, Kaplan A, Bloom A. Forthcoming. Marine radiocarbon calibration curve spanning 7000 to 50,000 years BP based on paired ^{230}Th/^{234}U/^{238}U and ^{14}C dates on pristine corals. *Quaternary Science Reviews*.

Friedrich M, Remmele S, Kromer B, Hofmann J, Spurk M, Kaiser KF, Orcel C, Küppers M. 2004. The 12,460-year Hohenheim oak and pine tree-ring chronology

from central Europe—a unique annual record for radiocarbon calibration and paleoenvironment reconstructions. *Radiocarbon*, this issue.

Guilderson TP, Southon JR, Brown TA. 2003. High-precision AMS ^{14}C results on TIRI/FIRI turbidite. *Radiocarbon* 45(1):75–80.

Guilderson TP, Cole JE, Southon JR. Forthcoming. Prebomb $\Delta^{14}C$ variability and the Suess effect in Cariaco Basin surface waters as recorded in hermatypic corals. *Radiocarbon* 47(1).

Hughen KA, Overpeck JT, Lehman SJ, Kashgarian M, Southon J, Peterson LC, Alley R, Sigman DM. 1998. Deglacial changes in ocean circulation from an extended radiocarbon calibration. *Nature* 391:65–8.

Hughen KA, Southon JR, Lehman SJ, Overpeck JT. 2000. Synchronous radiocarbon and climate shifts during the last deglaciation. *Science* 290:1951–4.

Hughen KA, Overpeck JT, Peterson LC, Trumbore S. 1996. Rapid climate changes in the tropical Atlantic region during the last deglaciation. *Nature* 380:51–4.

Indermuhle A, Monnin E, Stauffer B, Stocker TF, Wahlen M. 2000. Atmospheric CO_2 concentration from 60 to 20 kyr BP from the Taylor Dome ice core, Antarctica. *Geophysical Research Letters* 27:735–8.

Jones M, Nicholls G. 2002. New radiocarbon calibration program. *Radiocarbon* 44(3):663–74.

Kromer B, Friedrich M, Hughen KA, Kaiser F, Remmele S, Schaub M, Talamo S. 2004. Late Glacial ^{14}C ages from a floating, 1270-ring pine chronology. *Radiocarbon*, this volume.

Neftel A, Moor E, Oeschger H, Stauffer B. 1985. Evidence from polar ice cores for the increase in atmospheric CO_2 in the past two centuries. *Nature* 315:45–7.

Oeschger H, Siegenthaler U, Schotterer U, Gugelmann A. 1975. A box diffusion model to study the carbon dioxide exchange in nature. *Tellus* 27:168–92.

Paterne M, Ayliffe LK, Arnold M, Cabioch G, Tisnérat-Laborde N, Hatté C, Donville E, Bard E. 2004. Paired ^{14}C and $^{230}Th/U$ dating of surface corals from the Marquesas and Vanuatu (sub-equatorial Pacific) in the 3000 to 15,000 cal yr interval. *Radiocarbon* 46(2): 551–66.

Reimer PJ, Hughen KA, Guilderson TP, McCormac G, Baillie MGL, Bard E, Barratt P, Beck JW, Buck CE, Damon PE, Friedrich M, Kromer B, Bronk Ramsey C, Reimer RW, Remmele S, Southon JR, Stuiver M, van der Plicht J. 2002. Preliminary report of the first workshop of the IntCal04 Radiocarbon Calibration/Comparison Working Group. *Radiocarbon* 44(3):653–61.

Reimer PJ, McCormac FG, Moore J, McCormack F, Murray EV. 2002b. Marine reservoir corrections for the subpolar North Atlantic for the last 5700 years. *Holocene* 12(2):129–35.

Reimer PJ, Baillie MGL, Bard E, Bayliss A, Beck JW, Bertrand CJH, Blackwell PG, Buck CE, Burr GS, Cutler KB, Damon PE, Edwards RL, Fairbanks RG, Friedrich M, Guilderson TP, Hogg AG, Hughen KA, Kromer B, McCormac G, Manning S, Bronk Ramsey C, Reimer RW, Remmele S, Southon JR, Stuiver M, Talamo S, Taylor FW, van der Plicht J, Weyhenmeyer CE. 2004. IntCal04 atmospheric radiocarbon age calibration, 26–0 cal kyr BP. *Radiocarbon*, this issue.

Robinson LF, Henderson GM, Hall L, Matthews I, Adkins JF. 2004. Climatic control of riverine and seawater uranium-isotope ratios. *Science* 305 (5685):851–4.

Siani G, Paterne M, Michel E, Sulpizio R, Sbrana A, Arnold M, Haddad G. 2001. Mediterranean Sea surface radiocarbon reservoir age changes since the last glacial maximum. *Science* 294:1917–20.

Sikes EL, Samson CR, Guilderson TP, Howard WR. 2000. Old radiocarbon ages in the southwest Pacific Ocean during the last glacial period and deglaciation. *Nature* 405:555–9.

Southon JR, Rodman AO, True D. 1995. A comparison of marine and terrestrial radiocarbon ages from northern Chile. *Radiocarbon* 37(2):389–93.

Southon J, Kashgarian M, Fontugne M, Metivier B, Yim WWS. 2002. Marine reservoir corrections for the Indian Ocean and southeast Asia. *Radiocarbon* 44(1): 167–80.

Stuiver M, Braziunas TF. 1993. Modeling atmospheric ^{14}C influences and ^{14}C ages of marine samples to 10,000 BC. *Radiocarbon* 35(1):137–89.

Stuiver M, Burk RL, Quay PD. 1984. $^{13}C/^{12}C$ ratios in tree rings and the transfer of biospheric carbon to the atmosphere. *Journal of Geophysical Research* D89: 11,731–48.

Stuiver M, Pearson GW, Braziunas TF. 1986. Radiocarbon age calibration of marine samples back to 9000 cal yr BP. *Radiocarbon* 28(2B):980–1021.

Stuiver M, Reimer PJ, Bard E, Beck JW, Burr GS, Hughen KA, Kromer B, McCormac G, van der Plicht J, Spurk M. 1998a. IntCal98 radiocarbon age calibration. *Radiocarbon* 40(3):1041–83.

Stuiver M, Reimer PJ, Braziunas TF. 1998. High-precision radiocarbon age calibration for terrestrial and marine samples. *Radiocarbon* 40(3):1127–51.

Takahashi T, Broecker WS, Bainbridge AE. 1981. The alkalinity and total carbon dioxide concentration in the world oceans. In: Bolin B, editor. Carbon cycle modelling. *SCOPE* 16:271–86.

van der Plicht J, Beck JW, Bard E, Baillie MGL, Blackwell PG, Buck CE, Friedrich M, Guilderson TP, Hughen KA, Kromer B, McCormac FG, Bronk Ramsey C, Reimer PJ, Reimer RW, Remmele S, Richards DA, Southon JR, Stuiver M, Weyhenmeyer CE. 2004. NotCal04—Comparison/Calibration ^{14}C records 26–50 cal kyr BP. *Radiocarbon*, this issue.

Waelbroeck C, Duplessy JC, Michel E, Labeyrie L, Paillard D, Duprat J. 2001. The timing of the last deglaciation in North Atlantic climate records. *Nature* 412: 724–5.

APPENDIX

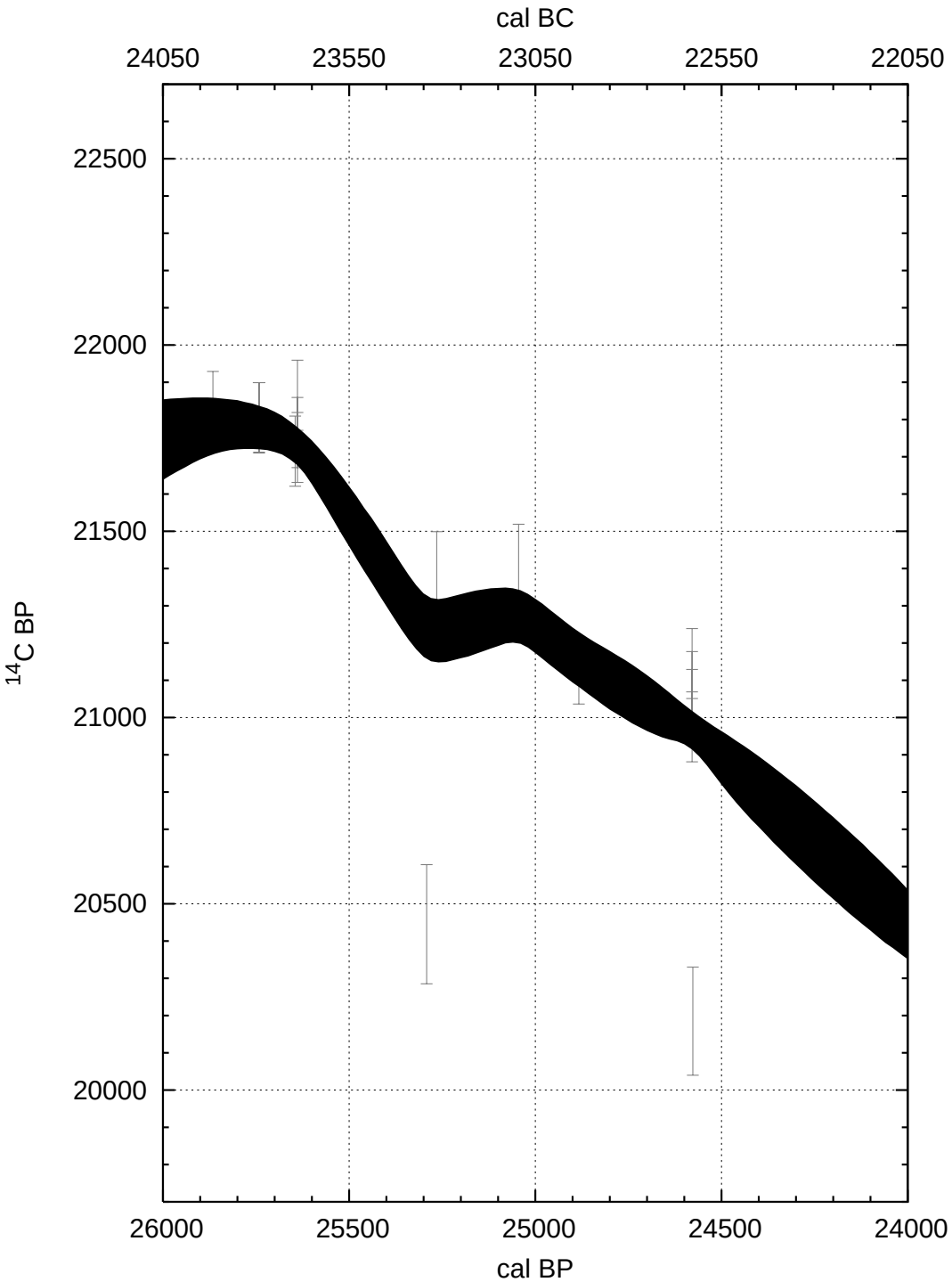

Figure A1 The Marine04 marine calibration curve (1-standard deviation envelope) and data with 1-standard deviation error bars increased by the laboratory error multipliers described in the text. The uncertainty in the calendar ages is not shown, but is taken into account in the random walk model.

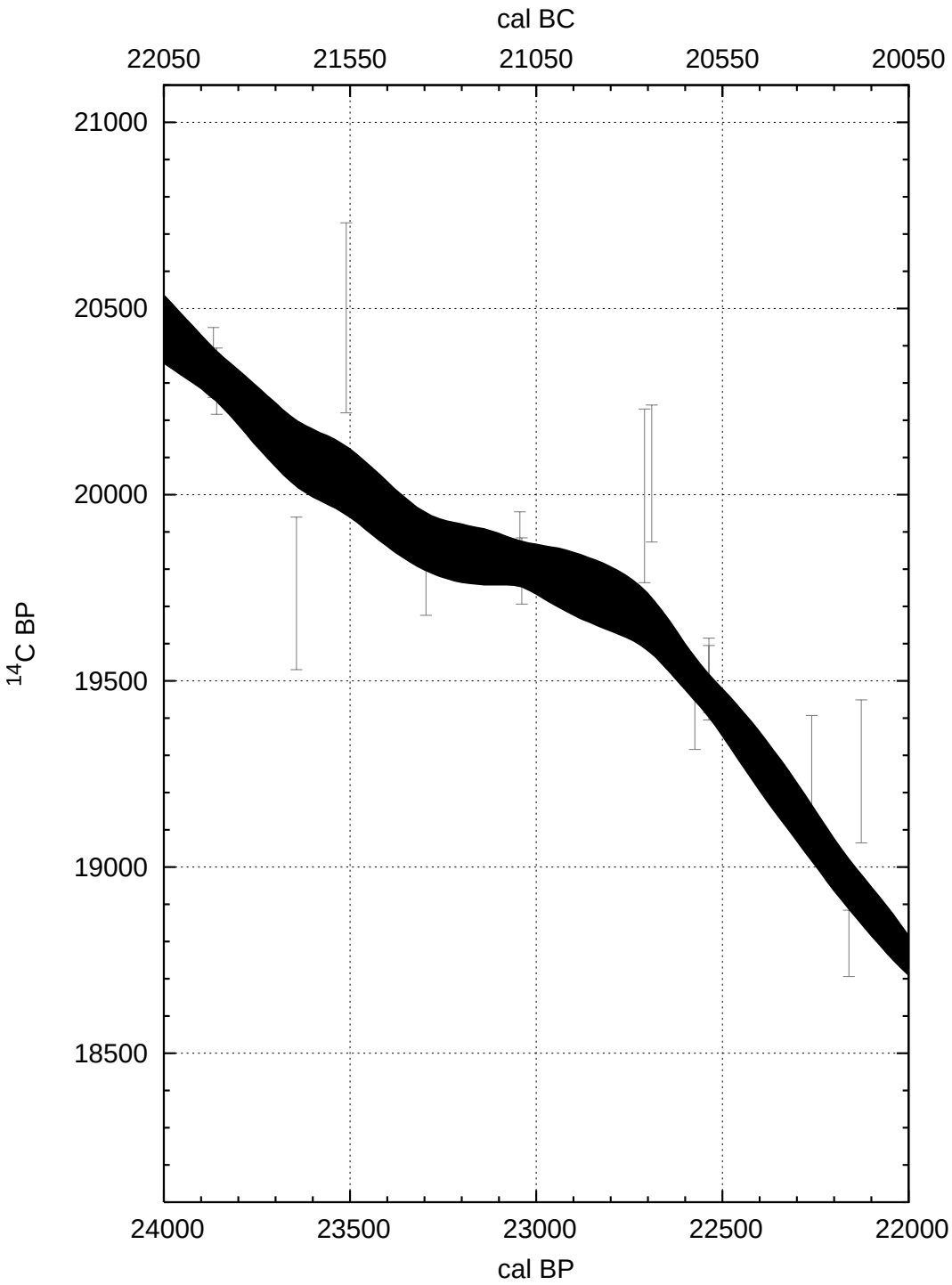

Figure A2 The Marine04 marine calibration curve (1-standard deviation envelope) and data with 1-standard deviation error bars increased by the laboratory error multipliers described in the text. The uncertainty in the calendar ages is not shown, but is taken into account in the random walk model.

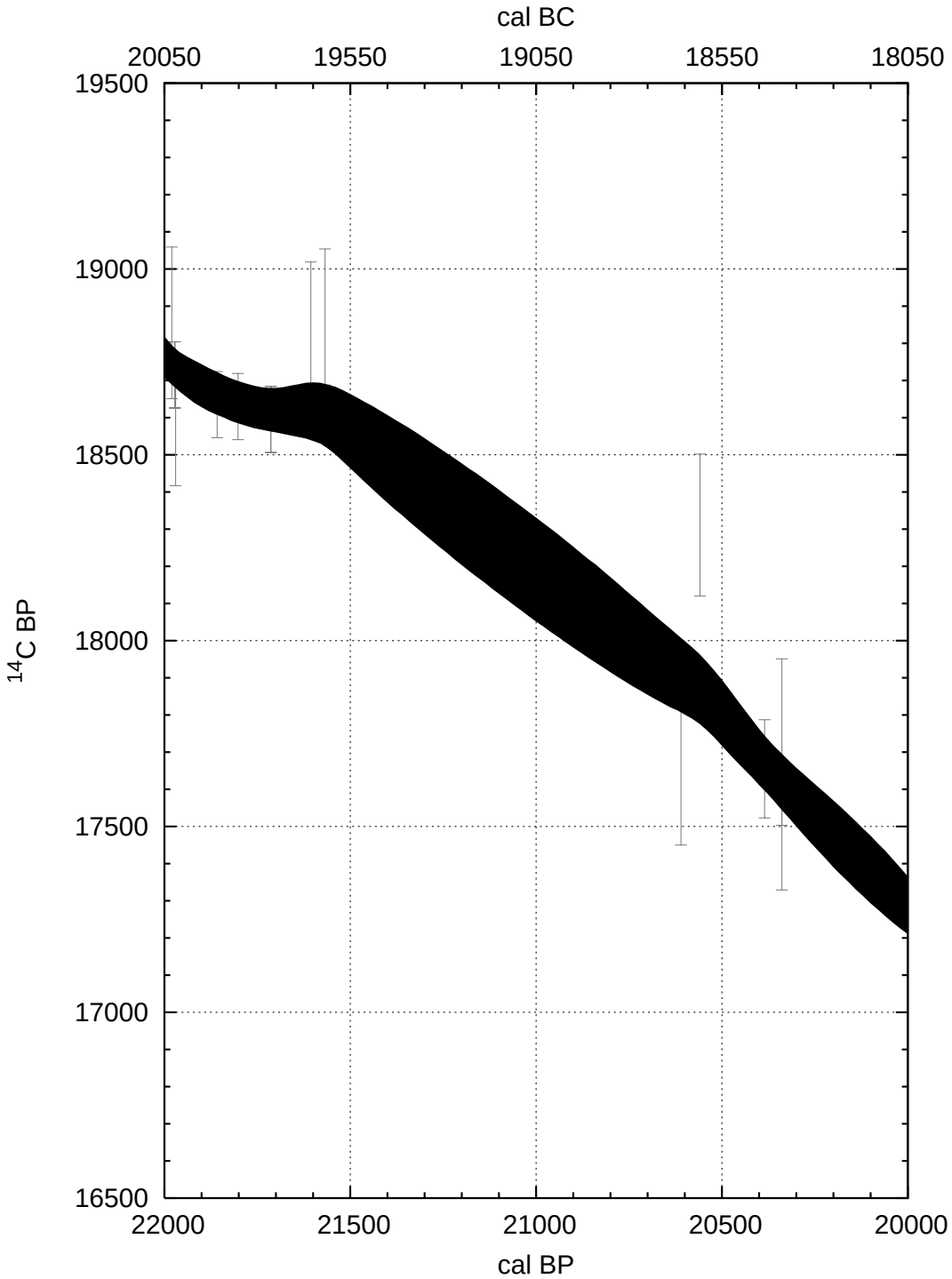

Figure A3 The Marine04 marine calibration curve (1-standard deviation envelope) and data with 1-standard deviation error bars increased by the laboratory error multipliers described in the text. The uncertainty in the calendar ages is not shown, but is taken into account in the random walk model.

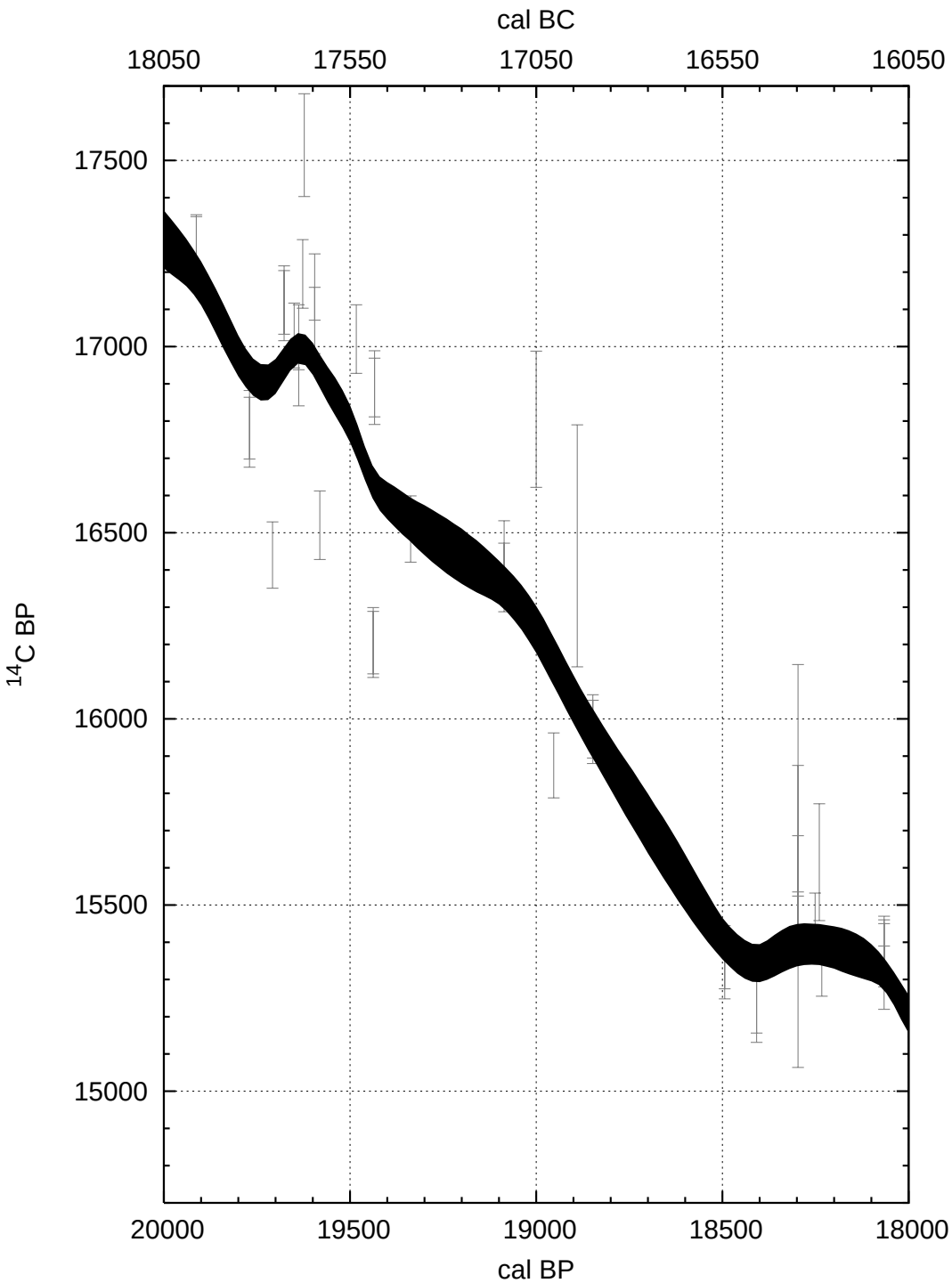

Figure A4 The Marine04 marine calibration curve (1-standard deviation envelope) and data with 1-standard deviation error bars increased by the laboratory error multipliers described in the text. The uncertainty in the calendar ages is not shown, but is taken into account in the random walk model.

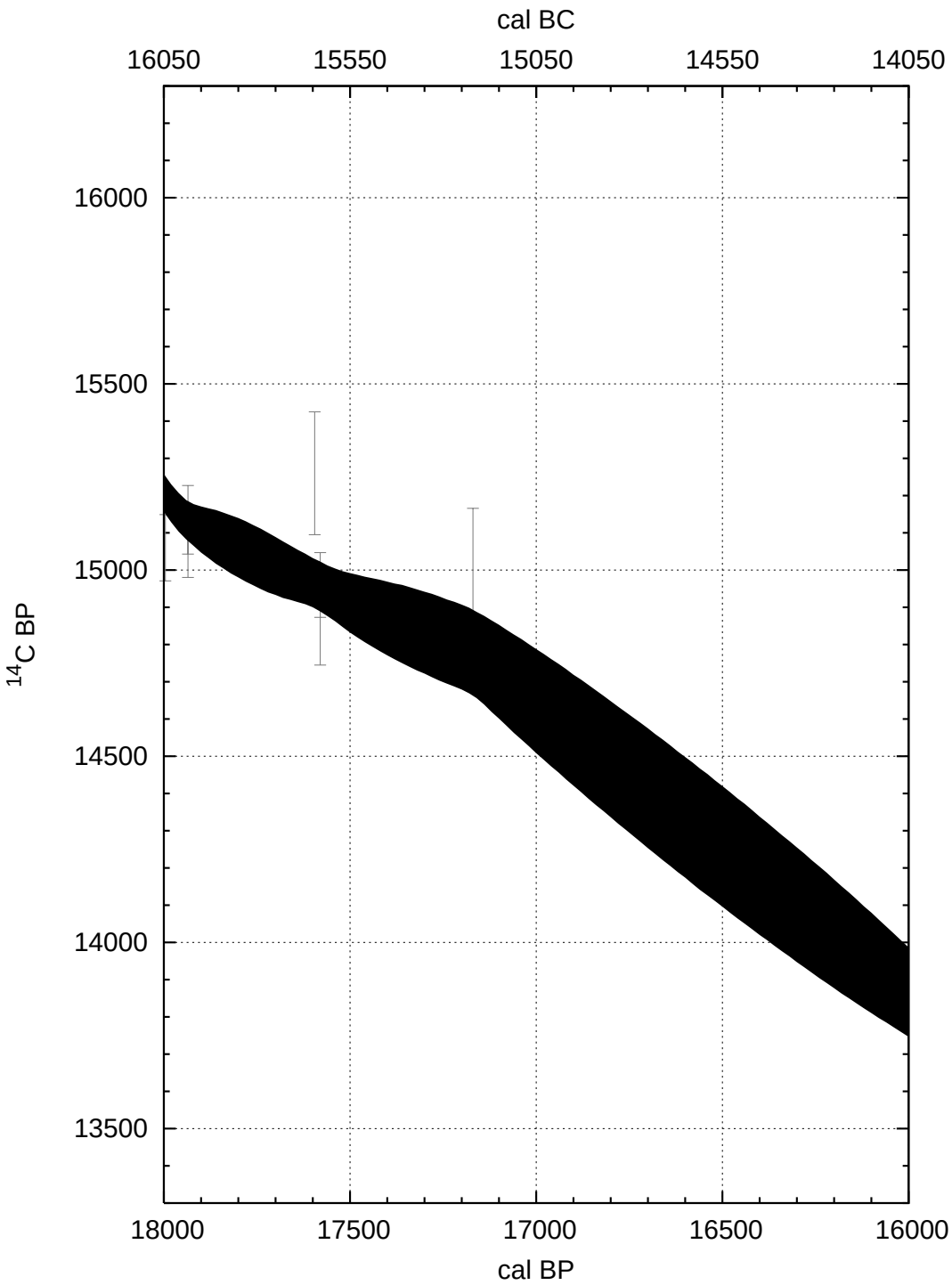

Figure A5 The Marine04 marine calibration curve (1-standard deviation envelope) and data with 1-standard deviation error bars increased by the laboratory error multipliers described in the text. The uncertainty in the calendar ages is not shown, but is taken into account in the random walk model.

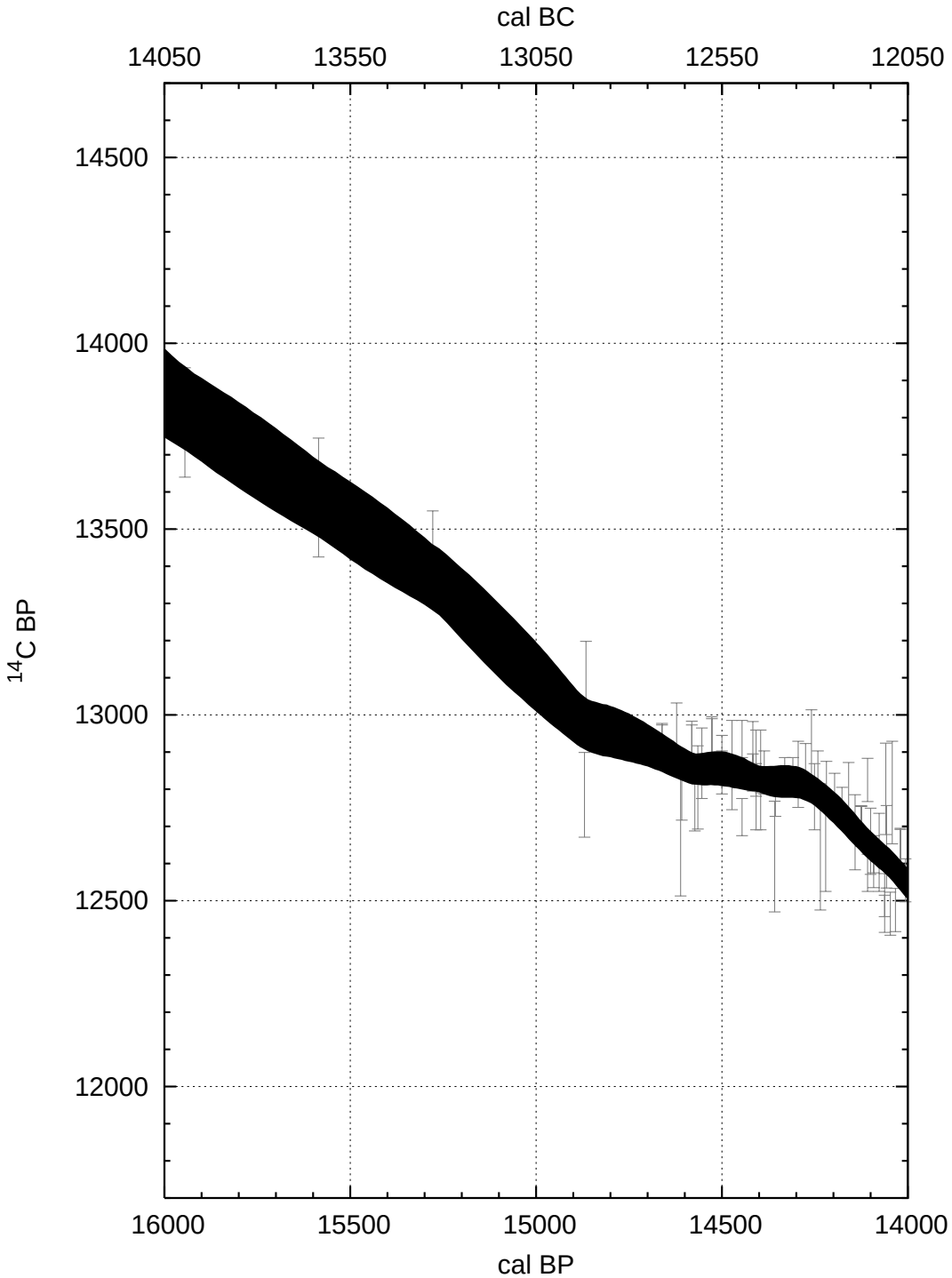

Figure A6 The Marine04 marine calibration curve (1-standard deviation envelope) and data with 1-standard deviation error bars increased by the laboratory error multipliers described in the text. The uncertainty in the calendar ages is not shown, but is taken into account in the random walk model.

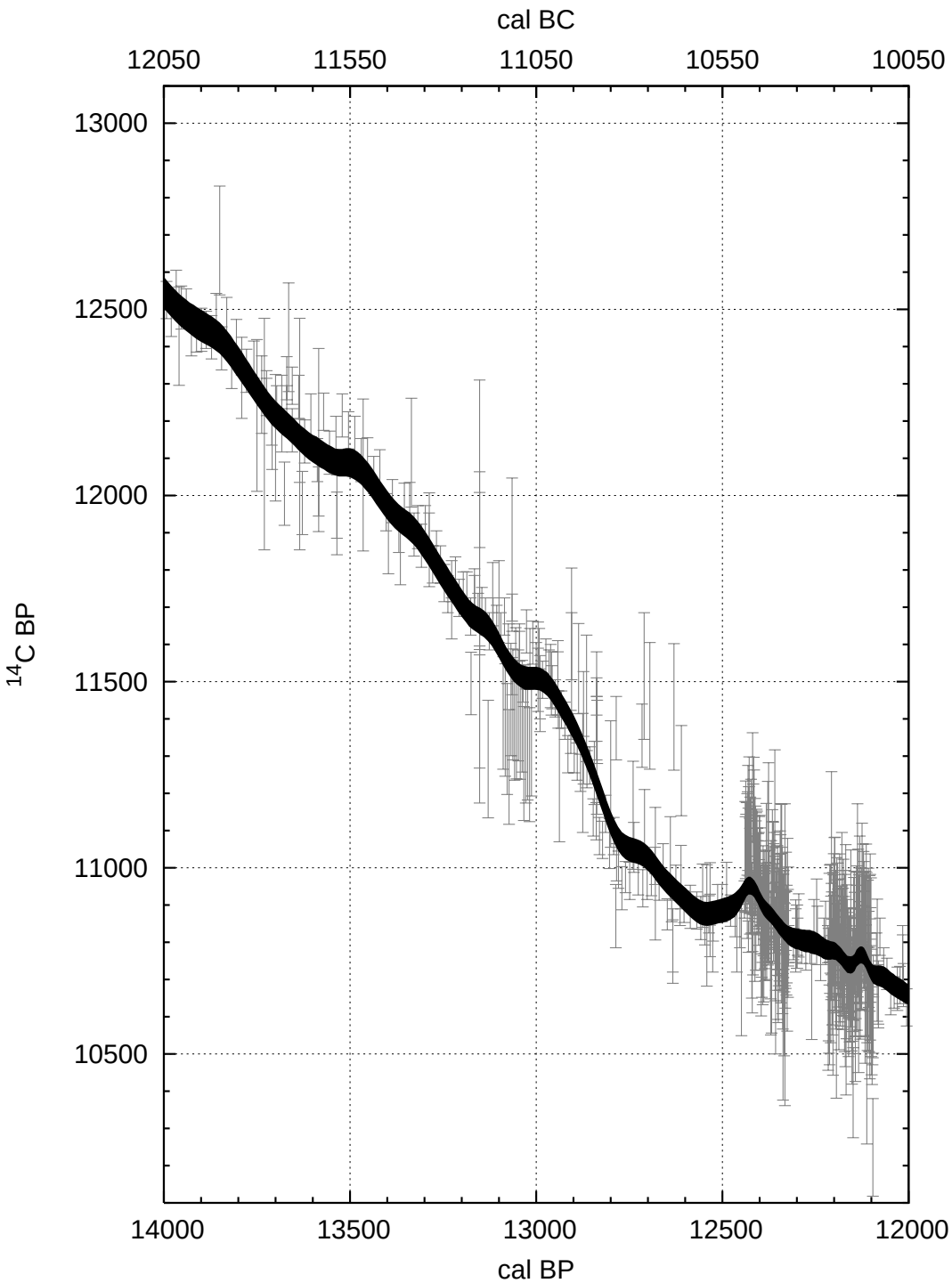

Figure A7 The Marine04 marine calibration curve (1-standard deviation envelope) and data with 1-standard deviation error bars increased by the laboratory error multipliers described in the text. The uncertainty in the calendar ages is not shown, but is taken into account in the random walk model.

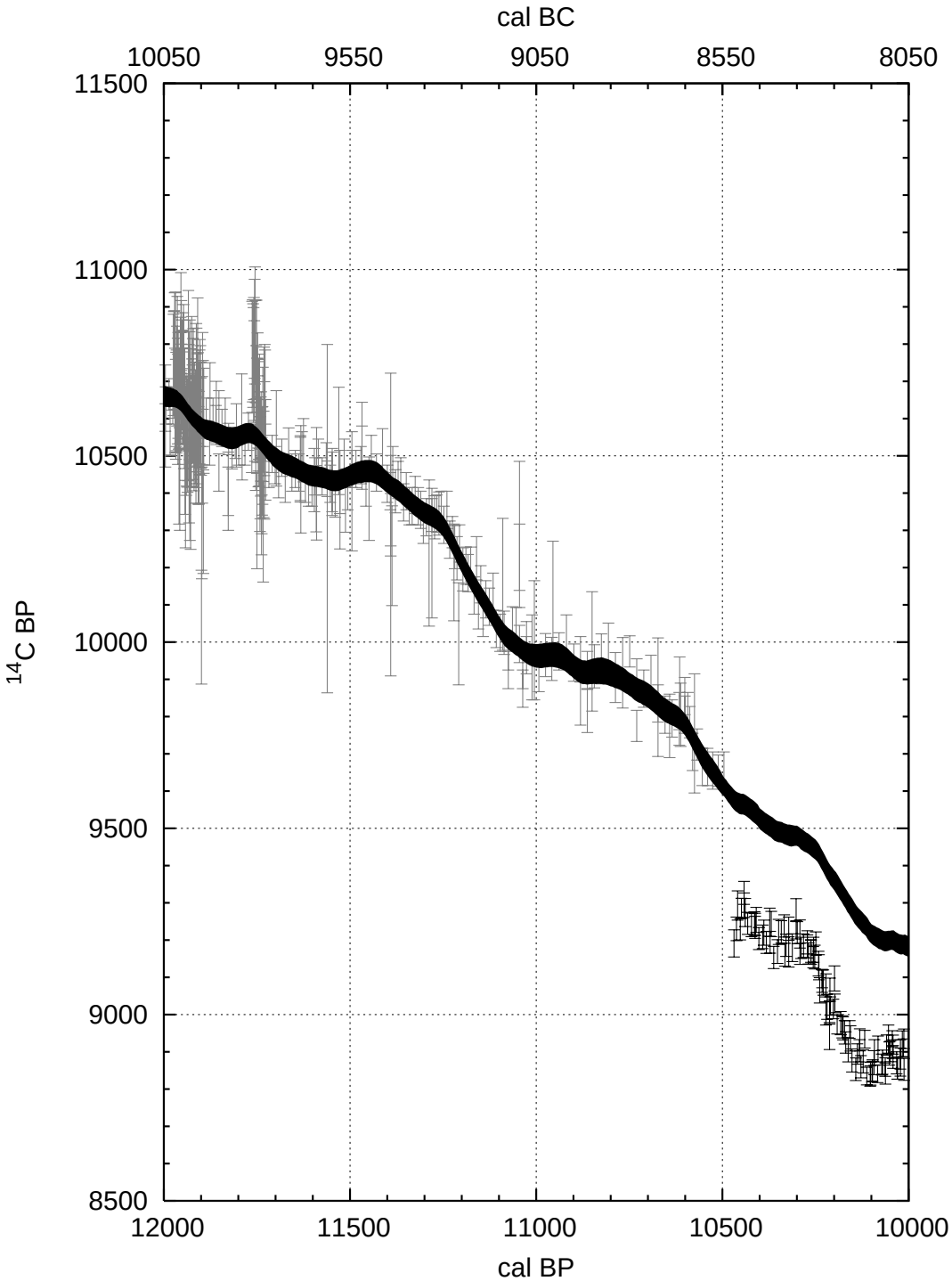

Figure A8 The Marine04 marine calibration curve (1-standard deviation envelope) and data with 1-standard deviation error bars increased by the laboratory error multipliers described in the text. The uncertainty in the calendar ages is not shown, but is taken into account in the random walk model.

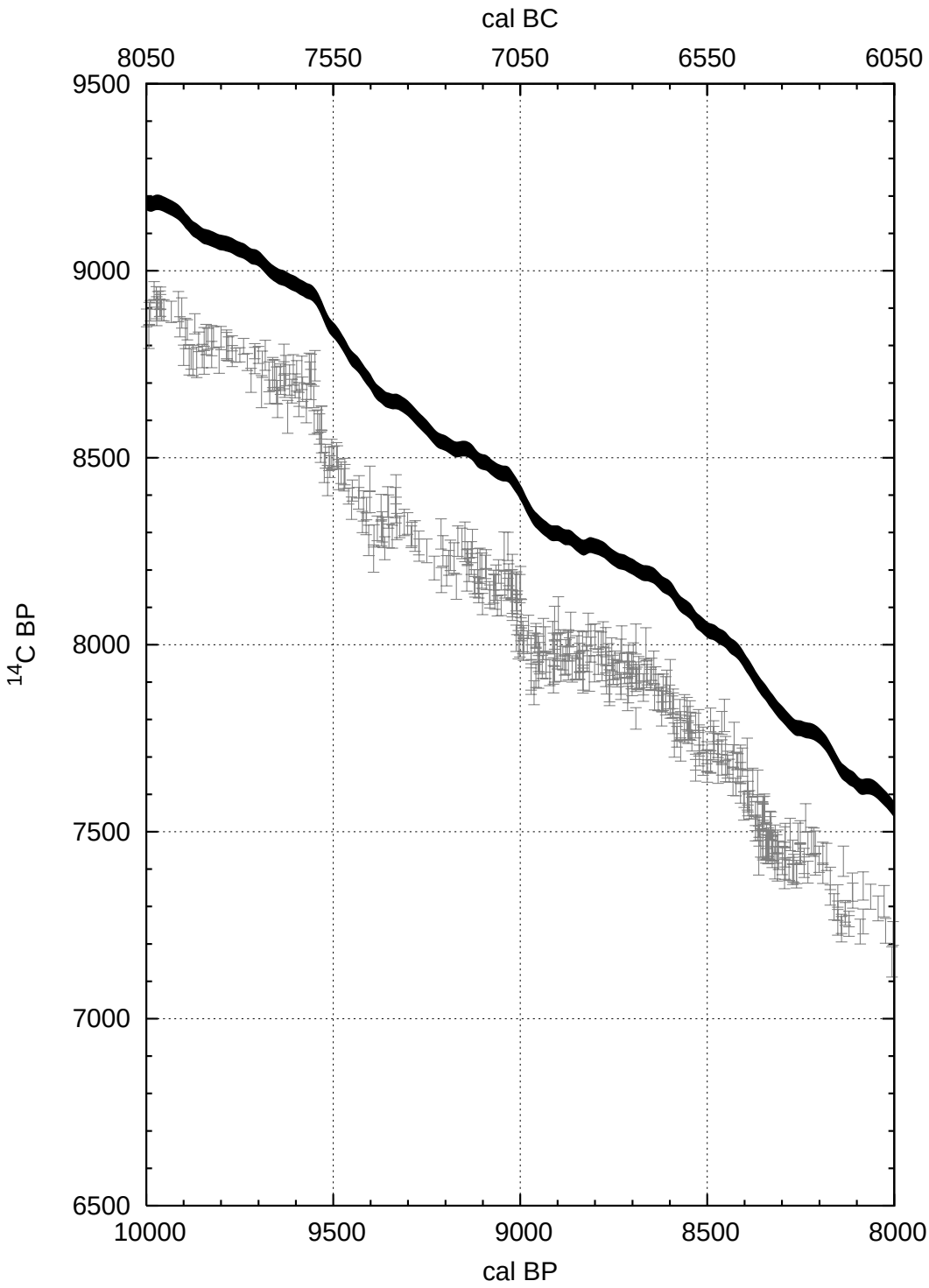

Figure A9 The Marine04 marine calibration curve (1-standard deviation envelope) and data with 1-standard deviation error bars increased by the laboratory error multipliers described in the text. The uncertainty in the calendar ages is not shown, but is taken into account in the random walk model.

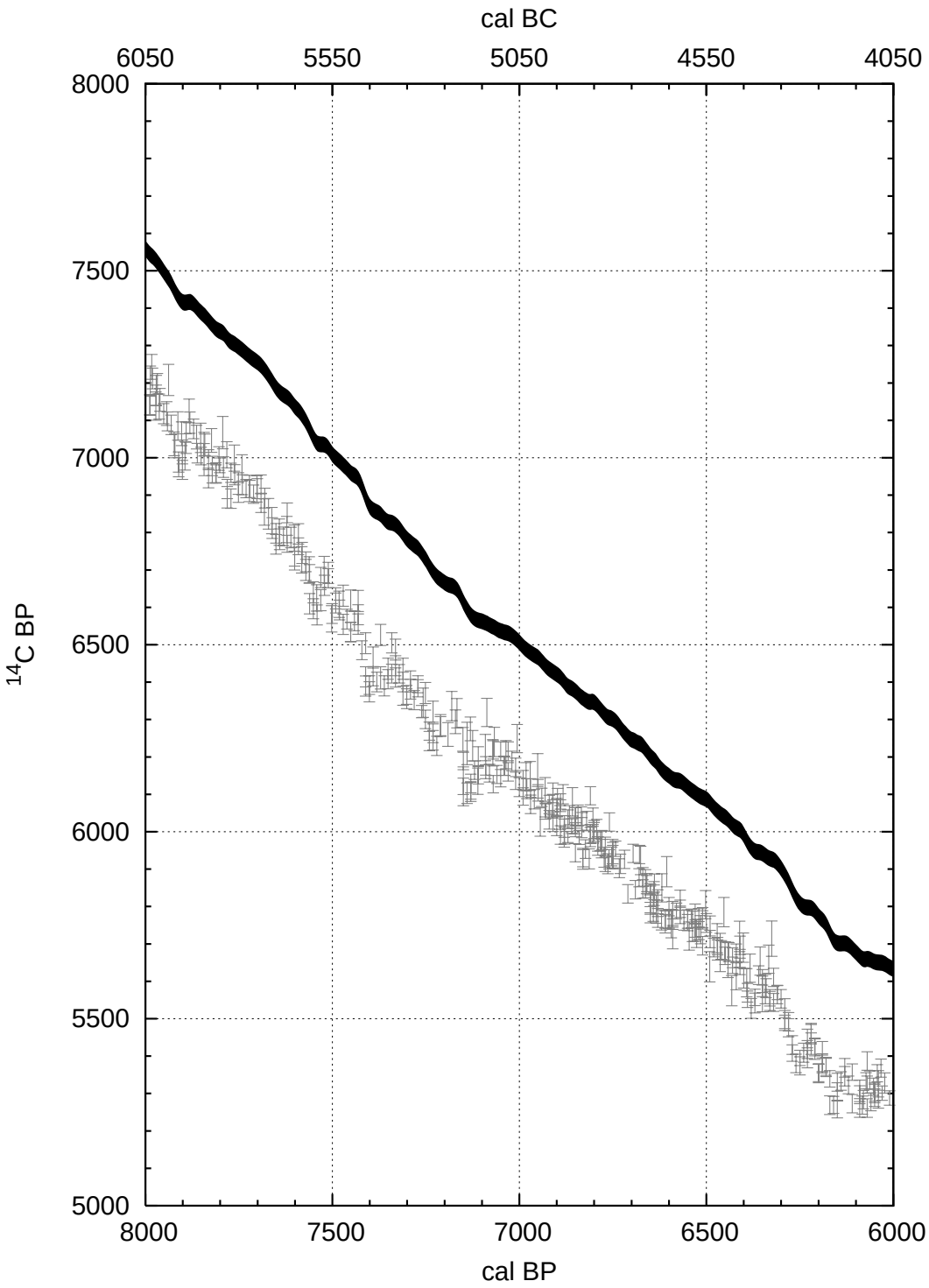

Figure A10 The Marine04 marine calibration curve (1-standard deviation envelope) and data with 1-standard deviation error bars increased by the laboratory error multipliers described in the text. The uncertainty in the calendar ages is not shown, but is taken into account in the random walk model.

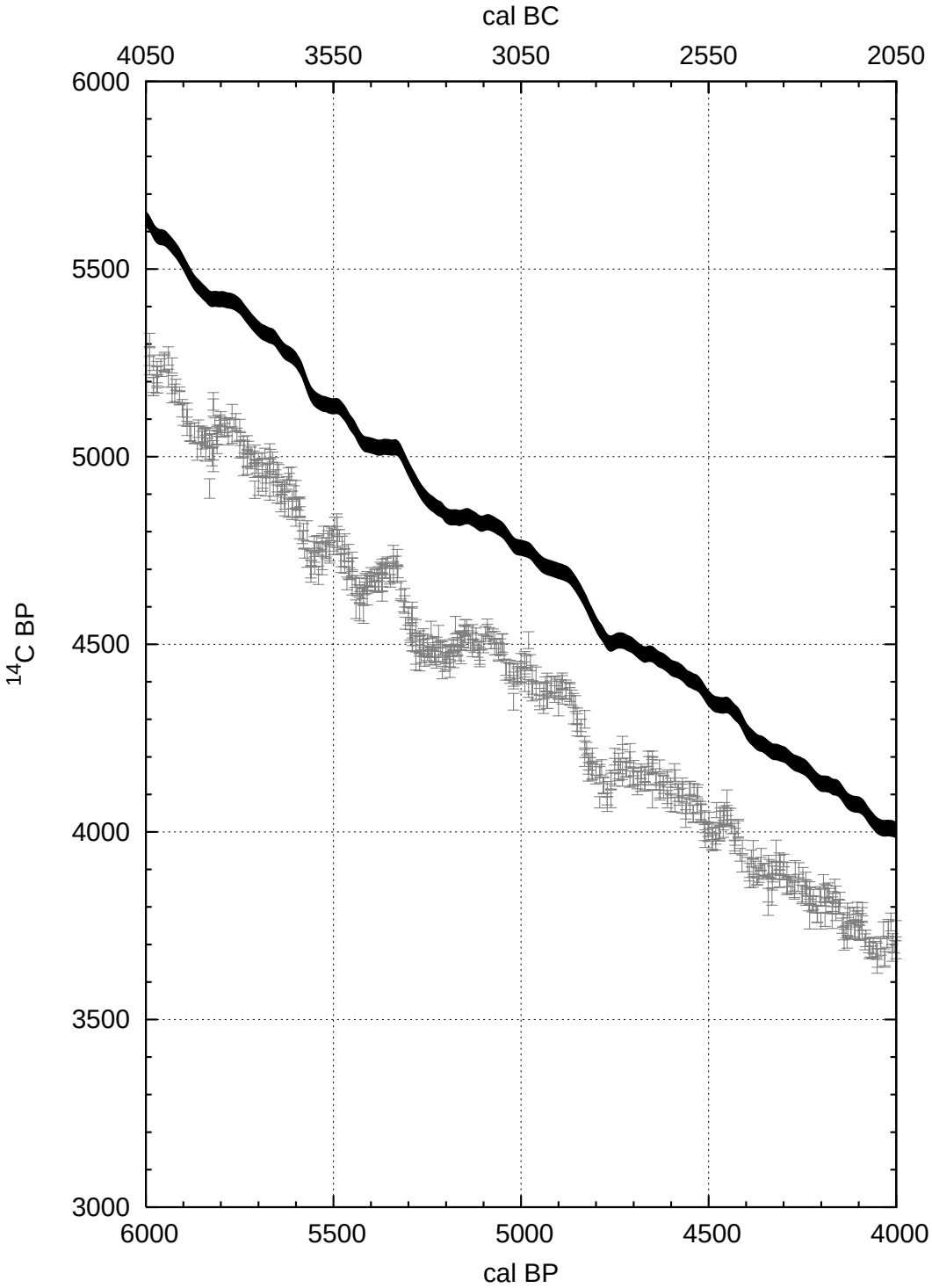

Figure A11 The Marine04 marine calibration curve (1-standard deviation envelope) and data with 1-standard deviation error bars increased by the laboratory error multipliers described in the text. The uncertainty in the calendar ages is not shown, but is taken into account in the random walk model.

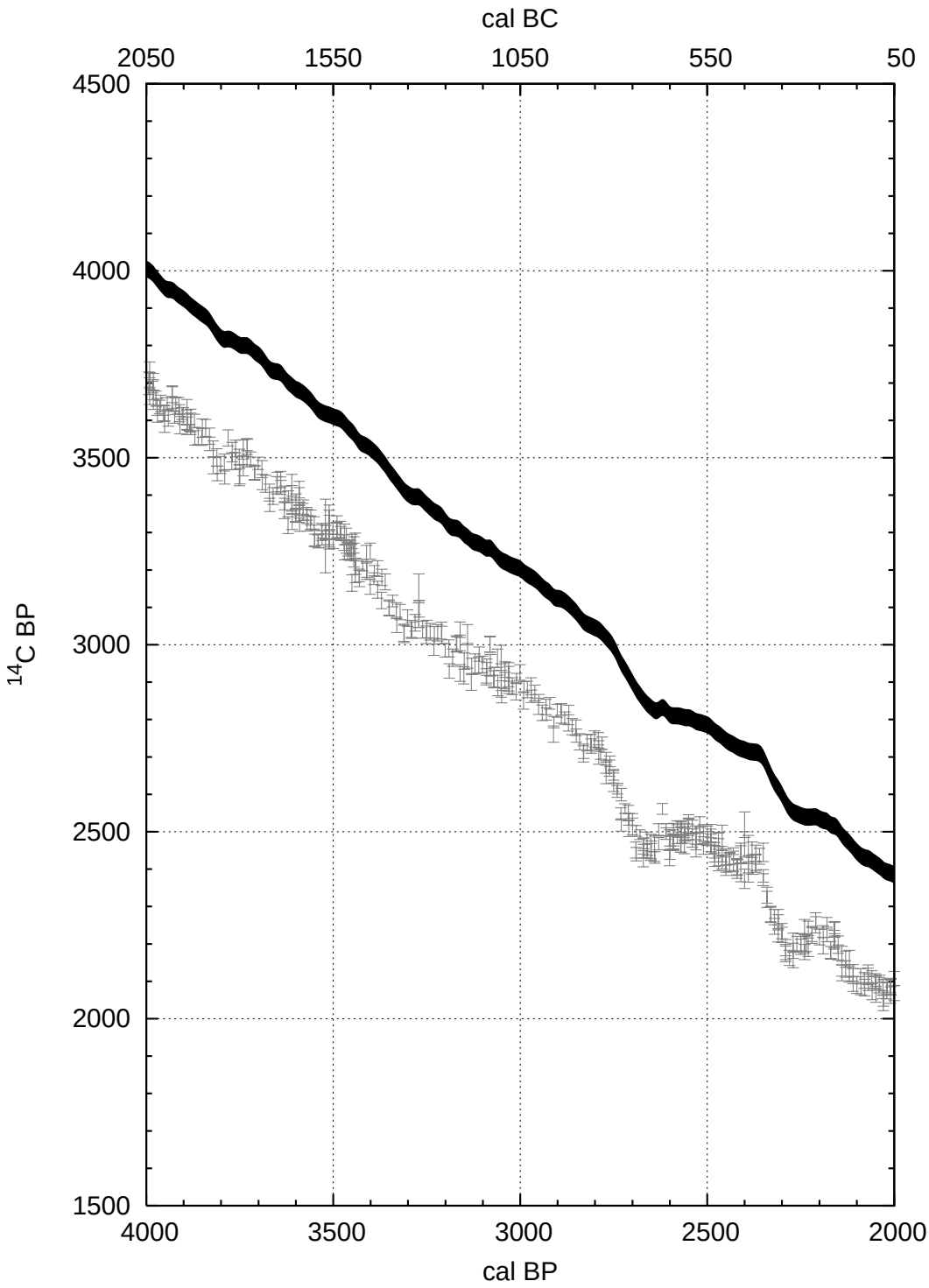

Figure A12 The Marine04 marine calibration curve (1-standard deviation envelope) and data with 1-standard deviation error bars increased by the laboratory error multipliers described in the text. The uncertainty in the calendar ages is not shown, but is taken into account in the random walk model.

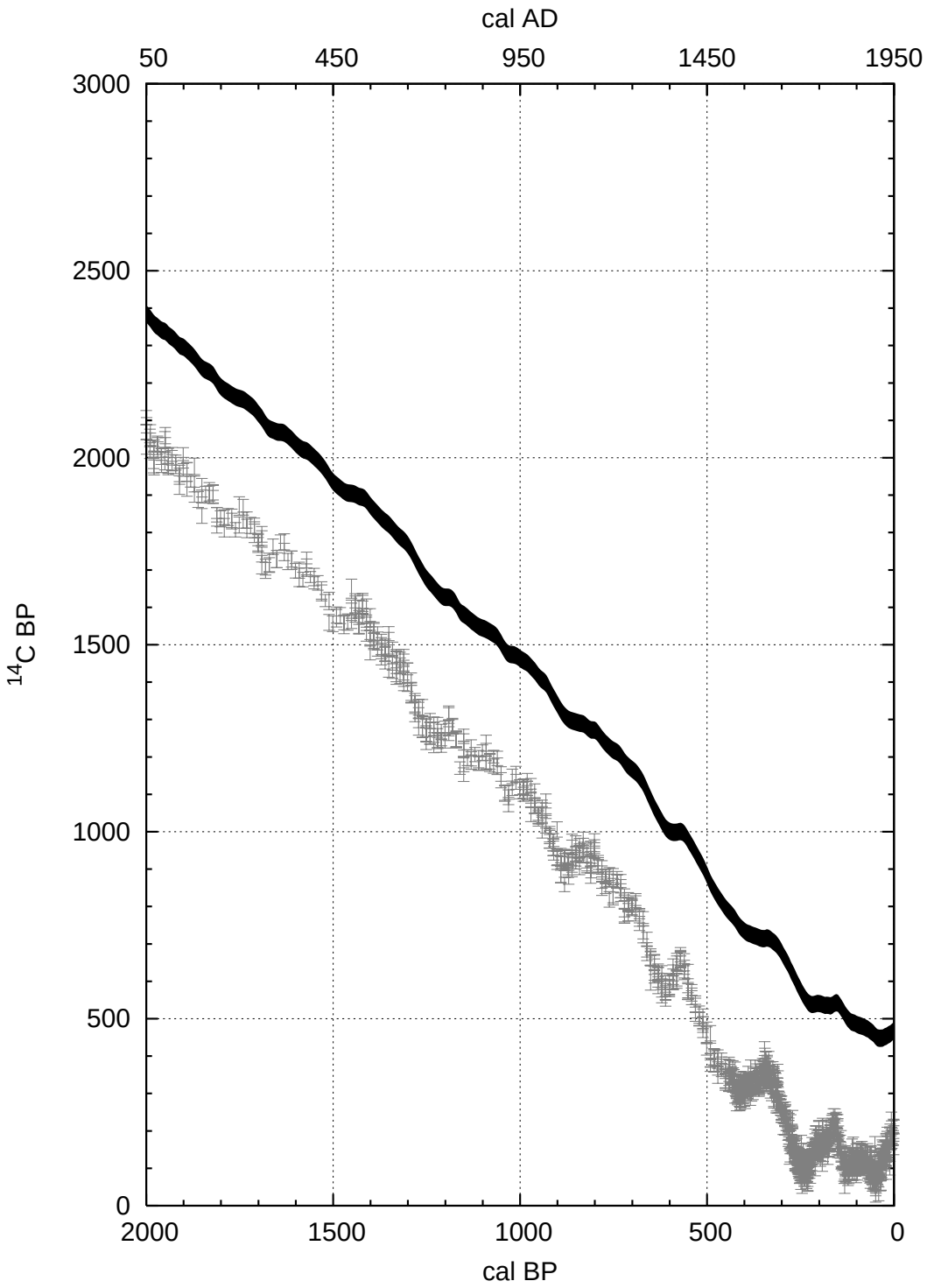

Figure A13 The Marine04 marine calibration curve (1-standard deviation envelope) and data with 1-standard deviation error bars increased by the laboratory error multipliers described in the text. The uncertainty in the calendar ages is not shown, but is taken into account in the random walk model.